The MECA Wet Chemistry Laboratory on the 2007 Phoenix Mars Scout Lander

Samuel P. Kounaves,[1] Michael H. Hecht,[2] Steven J. West,[3,4] John-Michael Morookian,[2] Suzanne M. M. Young,[1] Richard Quinn,[5] Paula Grunthaner,[2] Xiaowen Wen,[6] Mark Weilert,[2] Casey A. Cable,[1] Anita Fisher,[2] Kalina Gospodinova,[1] Jason Kapit,[1] Shannon Stroble,[1] Po-Chang Hsu,[1] Benton C. Clark,[7] Douglas W. Ming,[8] and Peter H. Smith[9]

[1] To analyze and interpret the chemical record, the 2007 Phoenix Mars Lander includes four wet chemistry cells. These Wet Chemistry Laboratories (WCLs), part of the Microscopy, Electrochemistry, and Conductivity Analyzer (MECA) package, each consist of a lower "beaker" containing sensors designed to analyze the chemical properties of the regolith and an upper "actuator assembly" for adding soil, water, reagents, and stirring. The beaker contains an array of sensors and electrodes that include six membrane-based ion selective electrodes (ISE) to measure Ca^{2+}, Mg^{2+}, K^+, Na^+, NO_3^-/ClO_4^-, and NH_4^+; two ISEs for H^+ (pH); a Ba^{2+} ISE for titrimetric determination of SO_4^{2-}; two Li^+ ISEs as reference electrodes; three solid crystal pellet ISEs for Cl^-, Br^-, and I^-; an iridium oxide electrode for pH; a carbon ring electrode for conductivity; a Pt electrode for oxidation reduction potential (Eh); a Pt and two Ag electrodes for determination of Cl^-, Br^-, and I^- using chronopotentiometry (CP); a Au electrode for identifying redox couples using cyclic voltammetry (CV); and a Au microelectrode array that could be used for either CV or to indicate the presence of several heavy metals, including Cu^{2+}, Cd^{2+}, Pb^{2+}, $Fe^{2/3+}$, and Hg^{2+} using anodic stripping voltammetry (ASV). The WCL sensors and analytical procedures have been calibrated and characterized using standard solutions, geological Earth samples, Mars simulants, and cuttings from a Martian meteorite. Sensor characteristics such as limits of detection, interferences, and implications of the Martian environment are also being studied. A sensor response library is being developed to aid in the interpretation of the data.

1. Introduction

[2] The 2007 Phoenix Mars Scout Lander will acquire and analyze samples of soil and ice to investigate the presence of water in all its phases and the historical record preserved in the chemistry and mineralogy of the regolith [*Smith et al.*,

2008]. It will also address biohabitability by identifying potential chemical energy sources available to support life, analyzing for organics, and identifying the potential of the geochemical environment to preserve paleontological evidence. The Microscopy, Electrochemistry, and Conductivity Analyzer (MECA) on board Phoenix, one of two primary soil analysis instruments, includes four identical Wet Chemistry Laboratories (WCLs) to address some of these objectives.

[3] The WCL cells, shown mounted in the MECA enclosure in Figure 1, will address the aqueous chemistry and reactivity of the Martian surface material. By measuring a variety of dust and regolith properties including pH, redox potential (Eh), solution electrical conductivity (EC), and soluble ionic species, we will be able to better understand or constrain Martian chemistry and mineralogy, the nature of Martian oxidants, the degree/nature of aqueous alteration, the potential for past or present biology, and potential hazards to human exploration. Combined with other Phoenix measurements, it will also allow us to better

[1]Department of Chemistry, Tufts University, Medford, Massachusetts, USA.
[2]Jet Propulsion Laboratory, California Institute of Technology, Pasadena, California, USA.
[3]Invensys Corporation, Foxboro Field Devices Division, Foxboro, Massachusetts, USA.
[4]Formerly at Thermo Fisher Scientific, Beverly, Massachusetts, USA.
[5]SETI Institute, Mountain View, California, USA.
[6]Thermo Fisher Scientific, Beverly, Massachusetts, USA.
[7]Lockheed Martin Corporation, Littleton, Colorado, USA.
[8]NASA Johnson Space Center, Houston, Texas, USA.
[9]Lunar and Planetary Laboratory, University of Arizona, Tucson, Arizona, USA.

Figure 1. Photograph of the MECA instrument package showing the placement of the four WCL units just prior to integration onto the Phoenix spacecraft deck at Lockheed Martin.

understand the aqueous, geochemical, and climatic evolution of the planet.

[4] Mars missions over the past three decades have consistently indicated that the surface of Mars has interacted extensively with liquid water in the past. Early visual observations from orbiters showed planetwide geomorphological features attributable to water [*Carr*, 1996]. Elemental composition of the Martian surface material by several landed missions has shown it to be predominately composed of silicon and iron but with significant levels of chlorine, bromine, and sulfur [*Clark et al.*, 1982; *Rieder et al.*, 1997; *Gellert et al.*, 2004; *Rieder et al.*, 2004]. Using elemental analyses and mineralogical models, the results are consistent with a regolith surface cover that contains 8–25% salts that are predominantly composed of NaCl and both $MgSO_4$ and $CaSO_4$ [*Clark and Van Hart*, 1981; *Catling*, 1999].

[5] The strongest evidence for episodic accumulations of liquid water on Mars has come from the Mars Exploration Rovers (MER) Spirit and Opportunity. In the Meridiani Planum region Opportunity has found evidence for groundwater activity in the form of sulfate-rich fluvial sediments that have undergone modification in the context of an aqueous environment and for evaporites formed in an arid environment with acidic groundwater [*Grotzinger et al.*, 2005; *Clark et al.*, 2005; *McLennan et al.*, 2005]. In the Columbia Hills at the Gusev site, Spirit has discovered patches of highly concentrated salt deposits [*Ming et al.*, 2006; *Squyres et al.*, 2006]. Although ferric sulfate is implicated as the predominant species in these deposits, accompanying salts include magnesium and calcium sulfates, as well as one sample implying the presence of an aluminum-potassium sulfate [*Yen et al.*, 2008]. Rare, large deposits of magnesium, calcium and polyhydrated sulfates have also been detected by infrared mapping spectrometry from orbit [*Bibring et al.*, 2005; *Murchie et al.*, 2007]. Calcium phosphates are also implicated in some Gusev materials [*Ming et al.*, 2006; *Clark et al.*, 2007] and minerals of this composition in Martian meteorites are soluble in weak acid [*Dreibus et al.*, 2000].

[6] Duricrusts at the Viking landing site were found to be enriched in magnesium sulfate [*Clark et al.*, 1982], as was regolith just below the surface in the Boroughs Trench at

Gusev [*Wang et al.*, 2006]. However, studies of a large number of unconsolidated soils at both MER rover sites, combined with results from Viking and Pathfinder, do not reveal either sulfur or chlorine bearing minerals. Indeed, variations of these species by as much as a factor of two are uncoupled from all other elemental variations (except Zn). This has led to the conclusion that globally distributed Martian aeolian material may have surficial coatings of volcanically emitted S and Cl species without stoichiometrically defined mineralizations [*Clark et al.*, 2006; *Yen et al.*, 2008].

[7] Despite the plethora of data from previous and ongoing missions, little is still known about the chemical reactivity of the Martian surface materials. Even though instruments have been previously proposed [*Clark et al.*, 1995; *Ming et al.*, 1998], and inferences made about the pH from the Viking GEX experiments [*Oyama et al.*, 1977; *Quinn et al.*, 2007], no direct measurement of pH has ever been made of Martian surface soil and there is no indication of what the ionic strength or identity of the soluble species when Martian soil is mixed with water will be. This knowledge is critical, both to help us understand the biological potential of Mars for supporting indigenous life in the past or present, and to assess hazards that may be encountered by future human explorers. Our current understanding is based entirely on measurements made on dry surface material via elemental analyses using either X-ray fluorescence, Mössbauer and optical spectroscopy, or optical microscopy.

[8] Since the Meridiani sediments are highly reworked and diagenetically modified, they most likely represent incomplete evaporitic layers that are not in equilibrium. Other observations that have yet to be explained include the unexpected distribution of sodium and potassium across minerals, the increasing concentration of chlorine in a zone where the sulfur concentrations begin to decrease, the possibility of unreacted acidic components in the cold, dry environment, and that the sulfur, bromine, and chlorine may also be present as sulfides, bromates and perchlorates, respectively [*Clark et al.*, 2005].

2. Science Objectives

[9] The 2007 Phoenix Mars Scout mission is dedicated to NASA's goals of studying life and climate. The mission's top two objectives are to study the history of the water at the landing site and to search for habitable zones. The interactions between sun, atmosphere, water, dust, and subsurface ice, in conjunction with the periodic changes of the ice/soil boundary, have most likely produced a unique chemical and mineralogical record in the regolith. The instruments on Phoenix will read this record and study the processes that control its distribution and phases. What is the origin of the ice layer, and how does it interact with the atmosphere? Once emplaced, has it gone through freeze–thaw cycles that affect ion mobility? How do local processes link with the global water cycle? Phoenix will also assess the biological potential of the near surface ice/soil mixture and determine its habitability. A habitable environment is one that is conducive to the growth of microbial life either continuously or at infrequent cycles. Does liquid water occur on Mars at the landing site that might sustain life? Are there

inorganic energy sources present in the soil that can sustain life? How hazardous is the environment to life as we know it or to future astronauts?

[10] As part of the overall Phoenix science goals, the specific objective of the WCLs is to characterize the aqueous chemical properties of soil samples as delivered by the Lander's robotic arm from the surface and at least two depths. To fulfill this goal, each WCL will determine the (1) hydrogen ion activity (pH), (2) redox potential (E_h/ORP), (3) solution electrical conductivity (EC), (4) concentration of selected soluble inorganic ionic species, and (5) possible redox couples and/or electrochemically mediated reactions.

3. Instrument Requirements

[11] The WCL science objectives have been translated into specific design requirements. Six of these pertain to the determination of inorganic ionic species and electrochemical properties, as follows:

[12] 1. The WCL is designed to measure the concentration of the anions Cl^-, Br^-, and I^- and the cations Na^+, K^+, Mg^{2+}, and Ca^{2+} in a particle-free aqueous solution with a pH from 3 to 10. To satisfy this requirement, it is necessary that the minimum detectable concentration be the greater of 10^{-5} M or 1% of the total ion concentration. It is also critical that in such solutions the presence of HCO_3^-, SO_4^{2-}, NH_4^+, Fe^{n+}, or other constituents of the leaching solution not interfere with the measurement.

[13] 2. The WCL is designed to detect SO_4^{2-} in solution at concentrations greater than 10^{-4} M and to determine its concentration at levels between 0.01 and 0.06 ± 0.01 M.

[14] 3. The WCL is designed to determine the pH of a sample/water mixture between pH 0–12 with an accuracy of ±0.5 pH units.

[15] 4. The WCL is designed to measure the reduction/oxidation potential between 1000 and −1000 mV with an accuracy of ±20 mV.

[16] 5. The WCL is designed to measure the electrical conductivity of the solution between 0.01 and 100 mS cm^{-1}.

[17] 6. The WCL is designed to run a cyclic voltammogram between ±1000 mV to an accuracy of ±1 mV.

[18] In addition, each WCL is designed to be able to perform these analyses for at least 90 min to study possible progressive changes as the liquid H_2O interacts with the soil, under agitation provided by a stirring motor. The WCL has the ability to monitor and control the temperature to ±1°C between 0 and 40°C, although most experiments are planned for the temperature range of between 5 and 10°C.

4. Instrument Description

4.1. Overview

4.1.1. Wet Chemistry Laboratory Fabrication

[19] The Mars Environmental Compatibility Assessment, a precursor to the Phoenix MECA package, was designed and built for NASA's Office of Human Exploration and Development of Space as a payload on the 2001 Mars Surveyor Program (MSP'01) Lander. This original MECA package contained four identical Wet Chemistry Laboratory units, each composed of an instrumented "beaker" assembly and an "actuator assembly." The purpose of the 2001 MSP

MECA and the WCL was to assess the hazards of the Martian dust/soil environment to future human explorers. The MSP'01 Lander was canceled 1 year before launch.

[20] New requirements and concerns about sensor lifetime led to a decision to build new beaker assemblies for the Phoenix MECA package and to modify the original actuator assemblies to enhance their capabilities. The new beakers include a sensor to monitor the barium titration of sulfate, as well as silver wire electrodes for chronopotentiometric determination of the halides (Cl, Br, and I) and a Pt chronopotentiometry electrode. These new sensors replaced ion selective electrodes (ISEs) for cadmium, sulfide, and one of three lithium reference electrodes. The perchlorate ISE was redesignated as a nitrate ISE. The conductivity sensor was replaced by a newer, more accurate version and the heating power of the beaker was approximately doubled to accommodate the colder polar environment of the Phoenix landing site in contrast to the equatorial MSP'01 mission. The beakers also contain sensors for dissolved oxygen and carbon dioxide, but quantitative results are not expected from these gas sensors because of lifetime issues.

[21] The upper actuator assembly consists of a sealed, titanium leaching solution reservoir (water plus ionic species for initial sensor calibration); a 1 cm^3 soil sample drawer designed to receive the soil through a screened funnel from the robotic arm while removing any excess soil and depositing it into the beaker; a stirrer motor with impeller; a reagent dispenser; and sensors for pressure and temperature. For Phoenix, the actuator assemblies have improved reagent dispensers that release five crucibles rather than one (a calibration standard, an acid, and three crucibles of barium chloride for sulfate titration), a new pressure sensor with a wider working range, and an external "funnel" to increase the sample collection area. None of the modifications required machining of the existing flight assemblies or changes to the electrical interface. A single WCL unit from different perspectives is shown in Figure 2 with major components labeled, and a cutaway view in Figure 3 shows the interior.

4.1.2. Implementation Rationale and Strategy

[22] A typical Earth based lab analysis for several cations and anions in a complex natural sample would most likely be undertaken via ion chromatography (IC). The chromatographic separation would simplify the analysis and remove interferent signals, but would require samples to be filtered prior to analysis to remove sediment and other particulate matter. However, resource constraints on a Mars mission, in terms of the extreme environments from launch to Mars surface operations, power, mass, and cost, precluded the use of complex electromechanical devices such as an IC. The only alternative for ion determination in an aqueous soil/water solution was the use of solid state, nonmechanical, ion selective electrodes and other electrochemical techniques. Even with the use of such sensors, it was still necessary to avoid increased manipulation of solutions and reagents. Thus, the often used methodology of adding reagents to eliminate interferents and to effect standard calibration, by necessity, resulted in a very simplified and conservative analytical process.

[23] Combining an array of rugged electrochemically based sensors, most of which are not specific but selective, allows for the determination of ionic species over a broad
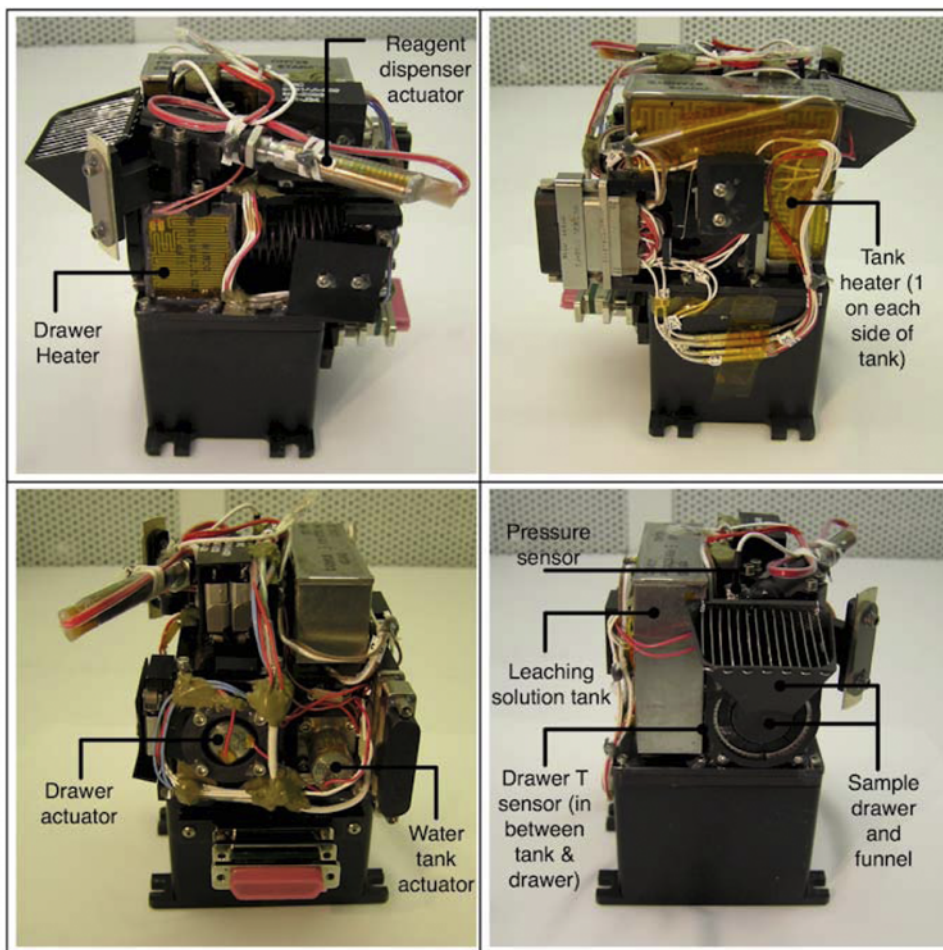
Figure 2. View of a single WCL showing location of the solution tank, reagent dispenser, funnel with soil screen, drawer, and beaker.

range of concentrations (10^{-5}–10^{-1} M) while at the same time, via use of chemometric methods, will give reasonably reliable quantitative information for individual species. The data provided by each ISE, in combination with the conductivity, pH, redox potential, and also the information provided by the differential scanning calorimeter and mass spec (TEGA) on Phoenix (W. V. Boynton et al., The Thermal and Evolved-Gas Analyzer on the Phoenix Mars Lander, manuscript in preparation, 2008), will allow a powerful set of tools to quantify and identify most ionic species that will most likely be encountered in a Martian soil sample.

4.2. Control and Communication

[24] Communication between MECA and the Phoenix spacecraft is through a serial interface, with commands originating at the Lander computer received by a field programmable gate array (FPGA) inside the MECA enclosure. The FPGA design is inherited from the MSP'01 mission, and is preprogrammed to acquire sensor data, to generate the waveforms necessary to run the various voltammetry and potentiometry scans, and to perform the basic actuator functions including temperature control. An additional electronics board dedicated to the WCL performs
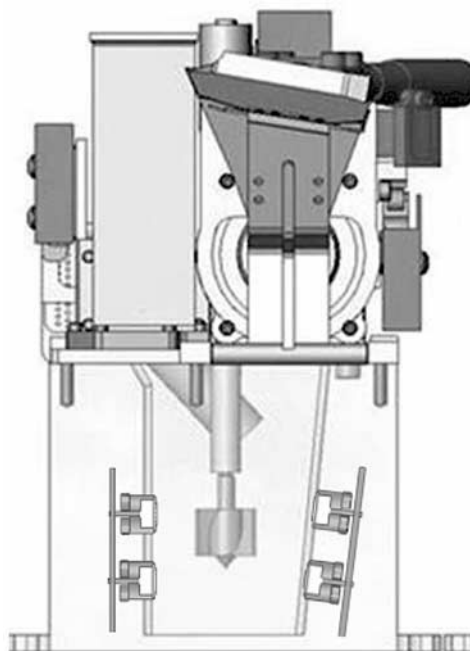

Figure 3. Cutaway view of the WCL showing location of stirrer and sensors.

Figure 4. Photograph of the open sample drawer showing the 1 cm^3 chamber for the sample. The brushes around the drawer entrance into the beaker remove excess soil.

all the necessary signal processing, including analog to digital and digital to analog conversion.

[25] As a result of buffer size constraints imposed by the serial interface, all waveforms must complete in approximately 10 s. This is adequate for CV and ASV, but is faster than desired for chronopotentiometry, which was not considered in the original design. The serial interface also constrains the sampling rate, and the returned data stream requires averaging over several seconds to achieve a satisfactory signal-to-noise ratio.

4.3. Actuator Design and Components

[26] The actuator assemblies (AA), mounted on top of the beakers, perform four primary functions; soil delivery, solution storage and delivery, reagent addition, and solution stirring. Designed and built by Starsys Research, Inc., each AA stores and delivers an aqueous solution into the reaction chamber; receives a sample from the robotic arm; delivers 1 cm^3 of soil to the chamber; seals the experiment from the Martian environment; and delivers crucibles filled with reagents for calibration, acidification, and sulfate titration. A motor drives an impellor to stir the solution when required.

4.3.1. Sampling and Drawer Operation

[27] Acceptance of the sample from the robotic arm and its addition into the beaker, containing the preinjected leaching solution, is accomplished by a paraffin-actuated drawer. The drawer when fully extended (shown in Figure 4 without funnel) protrudes approximately 2 cm from the face of the actuator. The funnel (Figure 2), whose purpose is to increase the collection area, has a cross-sectional area of approximately 8 cm^2 at the top, tapering down to an outlet area of approximately 1 cm^2. Strung across the top opening with a 2 mm spacing is a thin stainless steel wire that forms a sieve to prevent large sample particles from lodging in the drawer and preventing its closing.

[28] Since the WCL does not have the ability to determine the mass of the soil sample, we must rely on being able to visually estimate the volume of the sample in the 1 cm^3 drawer chamber (Figure 4). To accomplish this, an image of the drawer will be taken by the Robotic Arm Camera (RAC)

to provide some indication as to how well the chamber has been filled. Tests have shown that we can estimate the soil volume to 0.25 cm^3. However, even if the drawer could be reliably filled to exactly 1 cm^3, or the volume accurately determined, the density of the sample must still be estimated. Using knowledge of the surface materials at previously landed sites, and observations of the material initially observed or collected during the early surface phase of this mission, it should be possible to make a reasonable estimate of density, probably between 1 and 1.5 g cm^{-3}. Taking into account the worst cases of a small sample volume or an unexpectedly high or low density, the concentrations measured should still be within 50% of the actual levels.

4.3.2. Water Tank Assembly, Solution Deployment, and Operation

[29] Each WCL tank has a total volume of 36 mL and is filled with 26 mL of the leaching solution that is equilibrated with the headspace gas mixture of 0.8% CO_2, 94.2% N_2, and 5% He. The remaining 10 mL of headspace is filled with this gas mixture at room pressure ($\sim$1000 mbar). The gases in the headspace provide the pressure that will force the leaching solution into the beaker once the puncture disk is pierced under the reduced pressure conditions on Mars. The thin film heaters are used to melt the frozen leaching solution prior to solution deployment.

[30] The water tank assembly consists of a titanium tank with two external thin film heaters, a resistance temperature detector (RTD), and a puncture disk retained by a mechanical sealing system. To prevent galvanic corrosion, the puncture disk is coated first with titanium, then with parylene. A filled and sealed tank was subjected to accelerated lifetime testing and subsequent analysis of the tank solution showed no detectable trace metals from any component material. To verify the tank seal, the headspace gas composition included 5% He to enable leak testing of the final flight assembly. The leak rate was measured to be less than 0.5 cm^3 a^{-1} of headspace gas.

[31] During the cruise to Mars, the leaching solution in the tank will freeze and will remain frozen while on the surface of Mars. To use the solution, the tank heaters must be activated to thaw the solution. The thawing of the tank was tested against an environment of $-40°C$ and approximately 10 mbar pressure. Under such conditions the tank heaters are capable of completely melting the ice in the tank in 47 min, as shown in Figure 5.

4.3.3. Reagent Dispenser Assembly

[32] The reagent dispenser assembly (Figure 6) consists of a small chamber loaded with five crucibles, each containing a dry reagent. Figure 7 shows three of the crucibles which hold the barium reagent.

[33] The crucibles are made of alloy type 302 stainless steel and each holds a volume of $\sim$30 mm^3. The exteriors only are coated with 38 μm of Teflon® and a discontinuous film of Au/Pd alloy for charge control. Extensive testing retired the risk of chemical interaction between reagents and the stainless steel.

[34] The rate at which the reagent additions delivered in crucibles dissolve in the WCL beaker will affect the specification of beaker temperature as well as the time interval between reagent additions. To insure sufficient time for dissolution, the rate was measured using packed crucibles dropped into stirred beakers filled with leaching
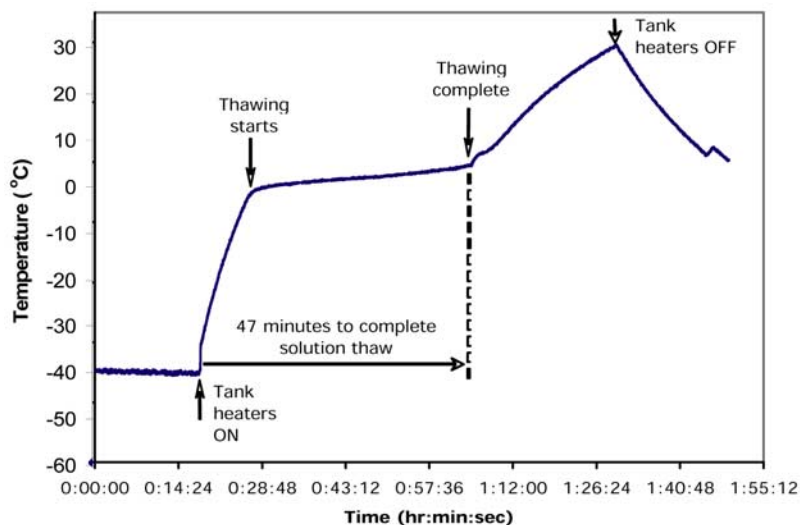
Figure 5. Plot of the tank solution temperature as the thin film heaters warm the frozen leaching solution. A WCL with a full tank was equilibrated to $-40°C$ in 10 mbar of pressure, followed by energizing the heaters with 10 W of power. Under this condition, 47 min were required to completely thaw the solution.

solution, as a function of temperature $(0-30°C)$ and pressures $(10-700$ torr$)$. Purging headspace gases from the beaker by opening and closing the sample drawer at least twice with the solution slightly above the solution boiling point $(\sim 6°C)$ helped eliminate trapped gases in the crucibles that might impede the dissolution of the contents. Successful deployment of partially filled crucibles using this methodology was demonstrated by monitoring the conductivity of a solution as crucibles with NaCl and 2-nitrobenzoic acid

were added into a solution at $5-7°C$ and Mars pressure $(\sim 8$ mbar $CO_2)$.

[35] The integrity of the reagents in the crucibles during long-term storage is a concern because the ISE hydrogels set the humidity level within the sealed WCL assembly. Although the loaded crucibles are not directly exposed to the beaker interior during the cruise to Mars, there does exist a pathway, albeit highly constricted, for water vapor exchange, thus creating the potential for water absorption by the reagents that causes swelling and possibly contamination of the crucible contents or jamming of the delivery mechanism. Barium chloride, in particular, is highly hygroscopic and will deliquesce if sufficient water vapor is
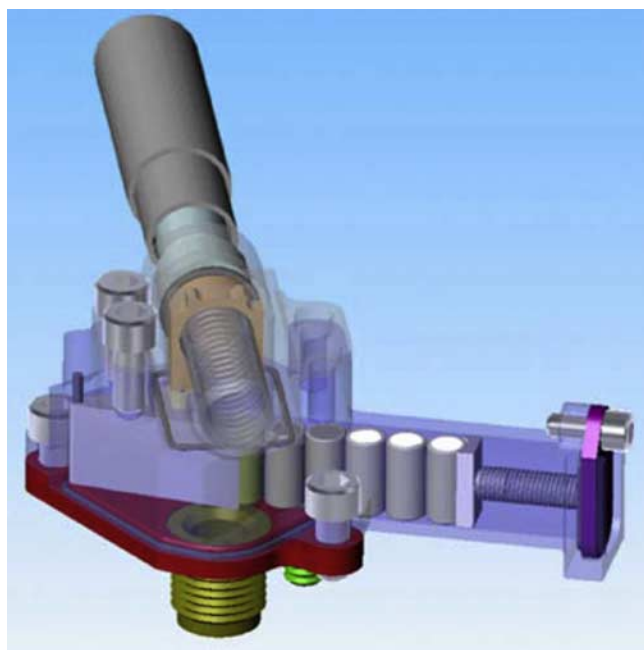
Figure 6. Diagram of the beaker reagent dispenser assembly showing five crucibles ready for deployment. Courtesy of SpaceDev.
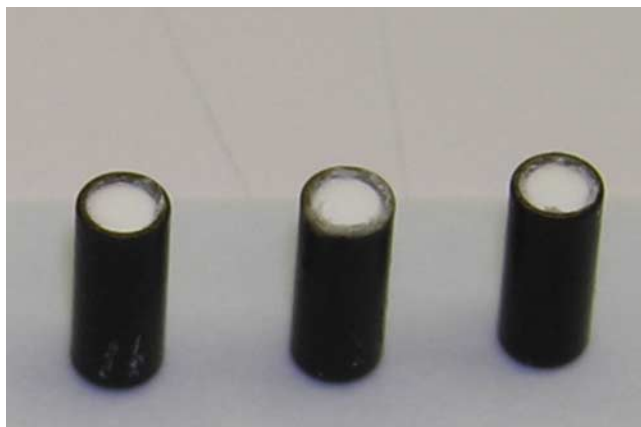
Figure 7. Photograph of $BaCl_2$-filled crucibles after 24 h in a WCL assembly filled with 25 mL of water. The entire assembly was held at $5°C$ and approximately 10 torr during the 24 h of exposure. No degradation of the $BaCl_2$ was observed, demonstrating that these crucibles will survive the $5-8$ h of exposure during Mars operation. The ragged edge along the top of the crucibles is the exterior Teflon® coating as it terminates at the top.

Figure 8. View of the sensors on two of the walls inside the WCL beaker.

present. The reagents were tested by exposing the filled crucibles to humidity levels within the sealed beaker for 14 days, after which time it was observed that the weight of the $BaCl_2$ had not increased and arguably had decreased, suggesting that the equilibrium condition between the ISE hydrogels and the $BaCl_2$ crucibles is such that the hydrogels retain their water, even possibly dehydrating the $BaCl_2$ with time. Within the accuracy of the weight scales used for the experiment, we estimate that the $BaCl_2$ storage life from the perspective of water absorption exceeds the 1.5 years of exposure from integration to the start of Mars operations by at least 2.5 years.

[36] The worse case water vapor exposure condition for the $BaCl_2$ crucibles actually occurs during Mars operation. During the WCL experiment, the beaker will contain leaching solution at a temperature of 5°C over 5–8 h of operation. Furthermore, the pressure inside the WCL assembly will be reduced (as high as ∼150 torr when the tank solution is first deployed; as low as ∼10 torr when the soil drawer is opened), which has the effect of exacerbating the water exposure relative to the Earth ambient pressure experiments. The survivability of the $BaCl_2$ crucibles was therefore tested under simulated experimental conditions for 24 h, 3 to 5 times the expected exposure time on Mars for a day of operations, then inspected for signs of water absorption by the reagents. As shown in Figure 7, no visible degradation of the $BaCl_2$ nor adverse impact on the crucible itself was observed.

4.3.4. Stirring

[37] The stirring assembly is designed to provide convection in the beaker during certain sample analyses. The stirring mechanism uses a miniature coreless dc motor to directly drive a shaft fitted on the end with a Teflon® mixing impeller (Figure 3). Depending on load, the motor rotates between 100 and 130 rpm.

4.4. Beaker Design and Assembly

[38] Except for the elimination and addition of several sensors, the WCL beaker assembly for the Phoenix was built-to-print using the MSP'01 mission beaker as the model. The theory, design, and demonstration of the components/sensors for that mission have been previously described [*Kounaves et al.*, 2003; *Lukow and Kounaves*, 2005].

[39] The beaker assembly, built by Thermo Fisher, consists of an inner cast epoxy beaker with a total cavity volume of 40 mL, and containing 26 embedded sensors (Figures 8 and 9). Between this inner beaker and the outer anodized aluminum casing are a set of printed circuit boards containing preamplifiers for each of the sensors (Figure 9). The solid-state sensors in the form of chips, pellets, or wires are bonded directly into the beaker walls flush with the inner wall of the beaker. Threaded rings mechanically retain the polymer membrane ISEs by compressing them against a lip in the beaker wall. The printed circuit (PC) boards containing the sensor preamps and some electronics are mounted on the outside and bottom of the inner beaker, with the sensor leads connected directly to the PC boards. Thin film heaters are installed between the beaker and circuit board at the bottom. The sensor and heater connections are routed via a flex circuit to a micro-D connector on the
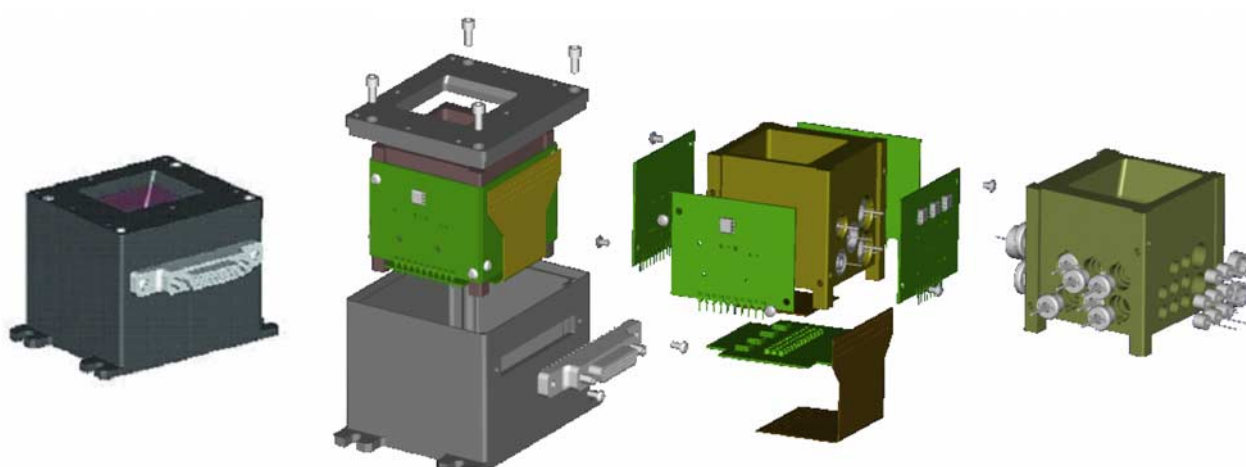

Figure 9. Diagram the individual components of the WCL beaker showing the sensors and electronics boards.
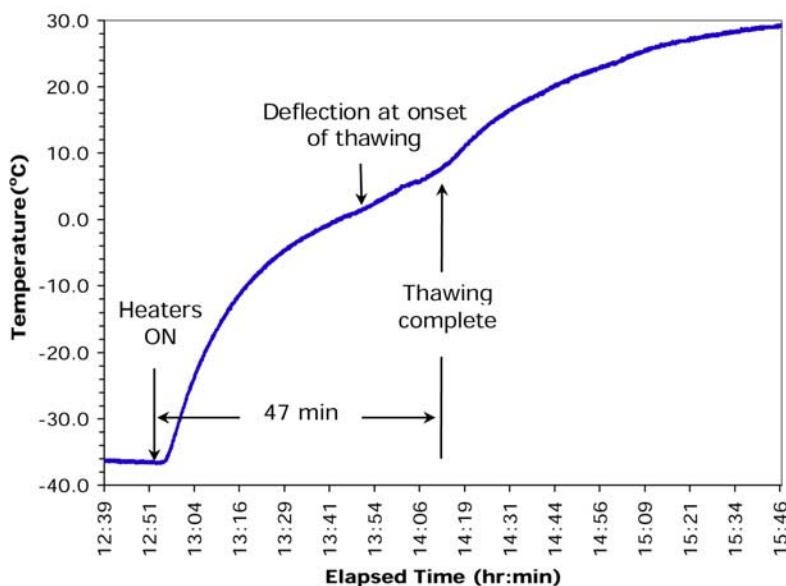
Figure 10. Plot of the beaker solution temperature as the beaker and drawer heaters warm the frozen leaching solution. Under the test conditions of −40°C and 10–50 torr of pressure, 25 mL of leaching solution was thawed in approximately 47 min.

aluminum housing. A lightweight potting compound fills the space between the inner beaker and the enclosure.

[40] Before final assembly and integration with the actuator, the inside surfaces of the beaker were washed several times with 18 MΩ sterile deionized water, rinsed with ethanol, washed again with water, dried with nitrogen gas, and finally all of the exterior surfaces were wiped with ethanol. Once the lower beaker and upper actuator assembly are integrated, the sensors will remain hydrated since the water present in the ISEs and that adsorbed by the reagents in the crucibles will come to a water vapor partial pressure equilibrium with only a fraction of the water in the sensors being used.

[41] The analytical protocol for soil analysis by a WCL unit requires that the solution in the beaker be allowed to freeze overnight (see section 7). Tests were conducted to verify the capability and survivability of the assembly under such a protocol. Figure 10 shows the thawing profile of a flight-lot assembly that was filled with 25 mL of leaching solution and allowed to equilibrate to −40°C under a pressure of 10–50 torr. The beaker temperature is measured with an RTD that is embedded in the beaker inner wall and exposed to the solution along with the chemical sensors. It was found necessary to energize both the beaker and drawer heaters to thaw the ice in the beaker and, under the conditions of the test, 47 min are required to completely thaw the solution. All of the sensors in the beaker walls were shown to be fully functional after the freeze/thaw cycle.

4.5. Beaker Sensors and Electrodes: Specifications and Theory of Operation

[42] Table 1 shows details of the 23 WCL sensors/electrodes mounted in the beaker walls. Not included on this list are a pressure sensor mounted for monitoring pressure in the headspace above the sample, and two temperature sensors,

all mounted in the AA unit that sits on top of the sensor beaker. In addition to the ISEs for inorganic ionic species, the beaker includes three sensors for pH, a carbon ring electrode for conductivity, a platinum electrode for redox potential, one platinum and two silver electrodes for chronopotentiometry, a gold electrode for cyclic voltammetry (CV), a microfabricated gold microelectrode array for ASV, and a temperature sensor.

4.5.1. Temperature and Pressure Sensors

[43] The temperature of each WCL unit is monitored by three temperature sensors, located on the drawer, tank, and beaker, all with a range of −50 to +70°C (±0.1°C). On the exterior of the water tank is a temperature sensor to determine when the water is fully melted, and hence when to actuate the water delivery system. A temperature sensor in the beaker is used for closed loop temperature control, including melting of ice for multiday experiments. A temperature sensor on the sample drawer is used to ensure that the o rings are sufficiently warm to maintain a seal while the drawer is in operation, and also serves to monitor temperature on the nearby reagent dispenser. Unrelated to the chemistry experiments, WCL electronics control an additional temperature sensor mounted on the microscopy stage.

[44] A pressure sensor is mounted on the actuator assembly in each WCL beaker to monitor the pressure in the beaker headspace (which includes the water tank after release of the leaching solution), and to measure any gas produced during the analyses. Manufactured by Kulite Semiconductor Products, Inc., the pressure sensor has a range of 0–1000 mbar with a sensitivity of slightly less than 0.1 mV mbar^{-1} (due to a wiring idiosyncrasy, one of the four sensors has a gain of ∼0.13 mV mbar^{-1}) and a compensated temperature range of −100°C to 40°C. The 11 bit digitization of the signal is in steps of approximately 3 data numbers per mbar, cutting off the high end of the

Table 1. Sensors in WCL Beaker[a]

	Sensor/Electrode	Type/Composition
1	Ammonium (NH_4^+)	ISE, PVC membrane doped with Nonactin
2	ASV (heavy metals)	564 12 μm Au disk microelectrode array (MEA)
3	Barium (Ba^{2+}) (used for SO_4^{2-})	ISE, PVC membrane doped with Ba ionophore-I
4	Bromide (Br^-)	ISE, solid pellet crystal
5	Calcium (Ca^{2+})	ISE, PVC membrane doped with ETH-1001
6	Chloride (Cl^-)	ISE, solid pellet crystal
7	Chloride REF	ISE, solid pellet crystal
8	CP (halides)	1-mm Ag disk electrode
9	CP (halides)	1-mm Ag disk electrode
10	CP (redox/acid/base)	1-mm Pt disk electrode
11	Conductivity	2-electrode (carbon rings)
12	CV (redox couples)	0.25 mm Au disk electrode
13	Iodide (I^-)	ISE, solid pellet crystal
14	Lithium 2 REF	ISE, PVC membrane doped w/Li ionophore-VI
15	Lithium 1 REF	ISE, PVC membrane doped with Li ionophore-VI
16	Magnesium (Mg^{2+})	ISE, PVC membrane doped with ETH-7025
17	Nitrate/perchlorate (NO_3^-/ClO_4^-)	ISE, PVC membrane doped with ion exchanger
18	ORP (Eh, redox potential)	1 mm disk platinum
19	pH	Iridium electrode coated with iridium oxide
20	pH 1	ISE, PVC membrane doped with ETH-2418
21	pH 2	ISE, PVC membrane doped with ETH-2418
22	Potassium (K^+)	ISE, PVC membrane doped with calinomycin
23	Sodium (Na^+)	ISE, PVC membrane doped with Na ionophore-VI

[a]REF is the reference electrode.

range slightly above 600 mbar. On assembly, both the head space in the sealed water tank and the interior of the beaker are at atmospheric pressure. During cruise to Mars the water tank maintains its pressure while the beaker is slowly vented through a calibrated leak. This arrangement allows the leaching solution to be delivered to the beaker by virtue of the positive pressure in the tank. During operation, the sampling drawer briefly allows pressure equilibration between interior and exterior as it is opened and closed, but not in either the fully open or fully closed position. This brief exposure is sufficient to purge gases other than water vapor from the chamber when the beaker temperature is at or above the external boiling point (approximately $5-7°C$ on Mars, depending on external pressure).

4.5.2. Ion Selective Electrodes

[45] The membrane ISEs, shown in Figure 11, are of the same design as the widely used commercial products, consisting of a housing, filling solution, membrane, and an internal reference electrode[*Fry and Langley*, 2002; *Frant*, 1997]. The ISE housings are made from the same material as the beaker. The internal filling solution is a hydrogel, composed of poly-2-hydroxyethyl methacrylate (poly HEMA) and an aqueous phase containing 10^{-3} M of the primary ion salt. In all cases, the chloride salt of the ion was used.. For the NO_3^-/ClO_4^- ISE, a mixture of 10^{-3} M NaCl and NH_4NO_3 was used. This ISE is slightly different from the other membrane ISEs in that it is based on the Hofmeister series of lipophilicity with a response for $ClO_4^- > I^- > Br^- > NO_3^- > NO_2^- > HCO_3^- > Cl^-$. Thus a significant concentration of perchlorate would overwhelm all responses to other anions. The membrane of each ISE is composed of about 30% polyvinyl chloride (PVC), plasticized with about $60-70\%$ of either ortho-nitrophenyl octyl ether (o-NPOE) or dioctyl sebacate (DOS), and doped with an ion-selective ionophore. The internal Ag/AgCl reference
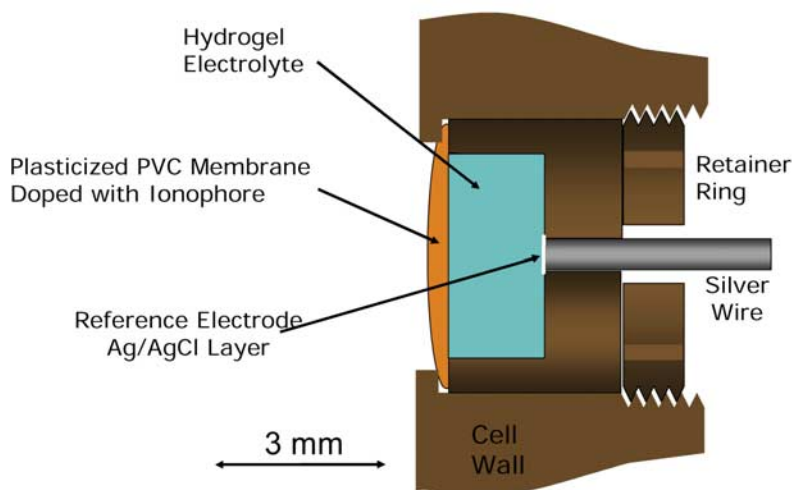

Figure 11. Diagram showing construction of a typical ion selective electrode (ISE).

electrode is made by chloridizing the exposed silver wire, thus coating it with a layer of AgCl.

[46] The basis for all ISE sensors is the measurement of a potential across an interface, the value of which is dependent on the concentration of a selected ionic species on each side of that interface. An external reference electrode is required to measure the potential across the ISE's polymer membrane. This has been accomplished in the WCL by using either of two Li$^+$ ISEs as a reference. The Li$^+$ ISE was chosen because of the low concentration of Li$^+$ expected in the Martian regolith and the high selectivity and stability of the Li$^+$ ISE. The leaching solution contains 10^{-3} M of Li$^+$ and thus the potential of the Li$^+$ ISE is expected to remain unchanged even after addition of the soil sample. The average Li$^+$ ISE potential versus a Standard Hydrogen Electrode (SHE) has been experimentally determined throughout the expected temperature range using a saturated Ag/AgCl reference as the SHE substitute.

[47] The selectivity toward a specific ion is dependent on the exchange reaction of the primary ion with the interface material such as a polymer/glass membrane, or a solid insoluble surface. Most of the ISEs used in the WCL are of the polymer membrane type with the exception of three for the halide ions. In a polymer based ISE, the membrane is responsible for the extraction of the primary ion from the aqueous sample into the organic membrane via a lipophilic ionophore that complexes with the ion at both the sample/membrane and membrane/hydrogel interfaces. The counter ion is excluded from the membrane due to the lipophilic salt in the membrane. As ions are extracted into the membrane, a potential difference develops across the two interfaces of the membrane that, when measured against an external reference electrode, is proportional to primary ion concentration in the sample. If only the primary ion is present in the sample solution, the response for the ISE can be predicted on the basis of the Nernst equation

$$E = E_i^\circ + (2.303RT/z_iF) \log(a_i), \qquad (1)$$

where E is the measured potential, E_i° is the standard potential of the electrode for ion i, R is the gas constant, T is the absolute temperature, F is Faraday's constant, z is the charge of ion i, and a is the activity of ion i. The slope of the E versus log (a_i) plot will give the sensitivity which is equal to $2.303RT/zF$ (59.2 mV/z) per tenfold change in the ionic activity. When $a = 1$, the intercept gives the standard potential, E°. Activity (a measure of the effective concentration of an ionic species) rather than concentration is always used with ISEs since as higher concentrations are approached, the two values deviate.

[48] The most important characteristic of a polymer membrane-based ISE is the ability of its ionophore to bind the primary ion when interfering ions of varied concentration are present in the sample. This is usually the case when the binding constant for the primary ion is several orders of magnitude greater than for the interfering ions. If however ions other than the primary one are present in the sample, the ISE may respond to the other ions and the Nernst equation will fail to accurately describe its response to the primary ion. In this case an extension of the Nernst equation, known as the Nikolskii-Eisenman equation, can be used to model the response of an ISE to its primary ion in a solution containing any number of interfering ions of the same or differing ionic charges. The potential is then given by

$$E = E_i^\circ + (2.303RT/z_iF) \log\left[a_i + \sum K_{ij}^{pot} a_j^{(z_i/z_j)}\right], \qquad (2)$$

where the subscripts i and j refer to primary and interfering ions and K_{ij}^{pot} is the potentiometric selectivity coefficient. This coefficient will be different for each interfering ion measured and describes the ability of the membrane to discriminate over interfering ionic species. The selectivity coefficient is commonly expressed as log K_{ij}^{pot}; the lower the value of the coefficient, the better the ionic discrimination. Since the selectivity coefficient for a given ionophore is not a constant but will vary depending on the overall membrane composition, experimentally determined rather than literature values are required for newly prepared membranes.

[49] Selectivity coefficients can be determined by several methods, however, the most often used is the separate solution method (SSM). The SSM uses the potential measured in a solution containing only the primary ion at a given concentration (E_i) versus the potential measured with the same electrode in a separate solution of only the interfering ion at the same concentration (E_j). The selectivity coefficient is then calculated using

$$\log K_{ij}^{pot} = \left[z_iF(E_j - E_i)/(2.303RT)\right] + \log\left[a_i/a_j^{(z_i/z_j)}\right] \qquad (3)$$

In using equations (1)–(3), there is an assumption that a theoretical Nernstian slope is expected for both the primary and interfering ions. In practice, ISEs often display theoretical slopes for the primary, but not the interfering ions. An interfering ion can only give a Nernstian slope if it can replace the primary ion from the membrane.

[50] If the ISE is exposed to a sample containing interfering ions to which it is weakly responsive, the primary and interfering ions will both participate in the ion exchange reaction thus preventing the accurate measurement of the interfering ions and producing a non-Nernstian slope. This is known as biased selectivity. To eliminate this bias, the ISE must be conditioned in a solution containing the interfering ion instead of the primary ion and then the SSM is used to calculate the selectivity coefficient. This method provides theoretical slopes for all ions and accurate selectivity coefficients. The unbiased selectivity coefficients can then be used to determine the expected error for a sample measurement. The minimum required selectivity coefficient or error can be calculated using

$$K_{ij}^{pot} = \left[a_i/a_j^{(z_i/z_j)}\right]\left[p_{ij}/100\right]^{(z_i/z_j)} \qquad (4)$$

where P_{ij} is the percent error. Using equation (4) is especially useful when an ISE is used in a sample containing an ion with a large interference (e.g., a Mg^{2+} ISE with a high Ca^{2+} interference).

4.5.3. Electrical Conductivity Probe

[51] The electrical conductivity of a solution is a measure of its ability to carry a current and is thus directly proportional to the total concentration of dissolved ionic species (e.g., Na$^+$, K$^+$, Ca^{2+}, Cl$^-$, SO$_4^{2-}$) in the water. The unit for
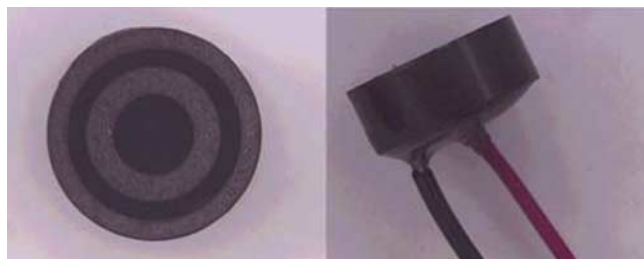
Figure 12. Image of the two carbon electrode conductivity probe.

EC is the siemens and is measured in microsiemens per centimeter (μS cm^{-1}). Conductivity is mainly affected by temperature and the nature of the ionic species. For the salts most likely to be found on Mars, the temperature is expected to produce about a 2% increase per 1°C. EC values are corrected and reported for 25°C and are technically referred to as specific electrical conductivity.

[52] Each of the conductivity probes (Figure 12) consists of a pair of activated carbon electrodes, a central 3 mm diameter disk surrounded by a 0.7 mm wide concentric ring 1 mm from the disk edge. The filler material between the electrodes is Stycast 2651–40 epoxy and the material of the outside encapsulation ring is "Z" epoxy. Electrical connections are made through the back side using silver epoxy. The cell constants for the EC electrodes used in the WCL are all approximately 1.45 cm^{-1}.

[53] In the WCL the EC is also used to calculate the ionic strength (μ), which is subsequently used to calculate the activity coefficient of the sample solution. The EC is converted to μ by using the experimentally derived equation $\mu = (7 \times 10^{-6})$ EC$^{1.0733}$. This equation was derived by using the measured value of the EC for the solutions shown in Table 2 and their calculated ionic strengths. This conversion assumes that the ionic mobilities of the selected ionic species are similar to those of ions that will carry the current in the sample solution. For samples with low concentrations of salts, this equation should suffice in providing a good estimate. If the sample contains salts at concentrations significantly higher than the test solutions or is of a significantly different composition (e.g., 25% sulfate), a new relationship will be derived by measuring the EC using a solution which more closely resembles the sample.

4.5.4. Oxidation Reduction Potential Electrode

[54] The oxidation reduction potential of an aqueous chemical system can be viewed as its "oxidizing power,"

i.e., its ability to transfer electrons. Following the International Union of Pure and Applied Chemistry (IUPAC) recommended convention, the term redox potential (E_h) is defined as the reduction potential at the standard electrode potential. The redox potential of a solution is normally measured at a platinum electrode in contact with the solution and is measured relative to a standard reference electrode, officially the standard hydrogen electrode (SHE). The presence of an oxidizing species such as peroxide is indicated by a positive potential while reducing substances such as sulfides produce a negative potential. If the redox couple is assumed to control the pH of a system, the redox potential can be expressed in terms of the modified Nernst equation as

$$E_h = E° + (0.059/n)\log(Red/Ox) - (0.059\ m/n)\text{pH} \quad (5)$$

where m is the number of hydrogen ions and n the number of electrons, involved in the reaction. As can be seen, E_h decreases with an increase in pH. When E_h is combined with pH, they define the conditions under which geochemical processes take place. In the WCL the redox electrode consists of a 1 mm diameter platinum disk and is referenced against the Li$^+$ ISE.

4.5.5. Hydrogen Ion Activity Electrodes

[55] The hydrogen ion activity of the soil water mixture is determined by three pH electrodes. Two of the electrodes are polymer-based ISEs and respond to H$^+$ ions in solution as described in section 4.5.2. The third pH electrode is fabricated by forming an iridium oxide layer (IrO$_2$) on an iridium substrate. The two ISE-based pH electrodes have an approximate dynamic range of 1 < pH < 9, while the iridium-based one has a range of 1 < pH < 12.

[56] During the initial design stages, there was uncertainty as to the survivability of the polymer-based aqueous gel ISEs for pH at extreme temperature and pressure and as to how many cycles of freezing and thawing, drying and rehydration, could be tolerated. As added redundancy for such a critical measurement as pH, a solid-state IrO$_2$ pH sensor was included. Uncertainty around the survivability of the polymer-membrane sensors has since been mitigated by several years of qualification testing, but the IrO$_2$ sensor still adds robustness to the WCL pH measurement capability.

[57] The IrO$_2$ layer pH electrodes, developed in the late 1980s, have several advantages over polymer and glass electrodes. These include good stability over a wide pH range and fast response time [Wang et al., 2002]. During

Table 2. Composition of Leaching and Testing Solutions

Solution Ionic Species	Concentration (M)					
	TS20 Leaching Solution (LS)	TS21 Test Calibrant Solution	TS22 Test Solution	TS23 Test Solution	TS24 Test Solution	M-TS21 Flight Calibrant Solution
Li$^+$	1.00E-03	1.00E-03	1.00E-03	1.00E-03	1.00E-03	1.00E-03
Na$^+$	1.00E-05	3.00E-05	1.10E-04	1.01E-03	1.00E-02	3.40E-05
NH$_4^+$	1.00E-05	3.00E-05	1.00E-04	1.00E-03	1.00E-02	3.40E-05
K$^+$	1.00E-05	3.00E-05	1.00E-04	1.00E-03	1.00E-02	3.40E-05
Ca^{2+}	1.00E-05	3.00E-05	1.00E-04	1.00E-03	1.00E-02	4.20E-05
Mg^{2+}	1.00E-05	3.00E-05	1.00E-04	1.00E-03	1.00E-02	3.47E-05
Ba$^+$	1.00E-05	3.00E-05	1.00E-04	1.00E-03	1.00E-02	3.80E-05
HCO$_3^-$	1.00E-05	3.00E-05	1.00E-05	1.00E-05	1.00E-05	3.40E-05
Cl$^-$	5.00E-05	1.50E-04	6.00E-04	6.00E-03	6.00E-02	1.90E-04
NO$_3^-$	1.03E-03	1.09E-03	1.30E-03	4.00E-03	3.10E-02	1.10E-03

testing all three electrodes gave similar values in the mid pH ranges. However, at less than about pH 4, the H^+ ISEs were more accurate, and at greater than about pH 9, the H^+ ISE became nonresponsive while the IrO_2 showed excellent response.

4.5.6. Cyclic Voltammetry Electrode

[58] Cyclic voltammetry (CV) will be used to search for the presence of soluble electroactive species in the Martian soil. In a CV experiment, the current at an electrode is measured as the potential is swept between two set voltages, with a reversal in scan direction occurring at a set switching potential. A detailed review of the technique is beyond the scope of this paper and reader is referred to the many texts that have been written which describe the theory and experimental practice of cyclic voltammetry [*Bard and Faulkner*, 2001].

[59] The mission requirement for the WCL is to perform CV between the set voltages of ±1 V relative to a Cl^- ISE. In the WCL implementation, as is typically done in laboratory experiments, a triangular waveform with a constant forward and reverse scan rate is used. A three-electrode configuration is employed, with the WCL platinum ORP electrode as counter electrode, a 250 μm diameter Au electrode as working electrode, and one of the chloride ISEs as reference electrode. The use of a WCL chloride ISE as the reference represents deviation from standard laboratory practice where a reference electrode with a constant and known potential is used. In the WCL, the potential of the reference electrode in each of four WCL cells will be a function of both electrode performance characteristics and the quantity of soluble chloride in the soil samples. Calculation of the electrode potential for each of the chloride reference ISEs will depend on their preflight calibrations and results of the ISE measurements made on Mars. Since the chloride concentration of the Mars soil samples is unknown, the potential window over which the CV electrode is scanned (±1 V versus Cl^- ISE) relative to a standard reference will not be known until after data from the WCL Sol A operations are returned to Earth. However, assuming Nernstian behavior, the potential of the chloride electrodes can be expected to vary linearly by about 170 mV over the concentration range from 1.5×10^{-4} M (concentration of Cl^- after addition of calibrants) to 0.1 M chloride in the sample solution.

[60] In a CV measurement, the level of current that flows between the working and counter electrodes depends on a number of factors including the concentrations of soluble redox active species. The WCL voltammetry circuit has six different gain settings to allow measurement over a broad range of current (i.e., concentration) levels. Since the measurement circuit does not have autoscaling capability, each CV scan will be repeated at each gain setting in order to cover the complete current range. As described in section 4.2, the spacecraft command interface constrains the total scan duration of a CV waveform to about 10 s, and the 4094 byte buffer limits the maximum number of data points for a single scan to 2015. Since the minimum potential step for the waveform is 1 mV, the combined effect of these two constraints is a minimum scan rate of about 333 mV s^{-1} for a complete cycle over a ±1 V window. Therefore, the nominal surface operation plan is to perform CV at a scan rate of 333 mV s^{-1} and two additional (higher) scan rates.

This means that a complete CV measurement cycle will require 18 scans (6 gain settings and three scan speeds). In some cases, (e.g., prior to addition of a Mars soil sample) fewer than 6 gain settings may be used to limit the number of electrode scan cycles. A full ±1 V triangular ramp will require 2 DAC steps with 3.2 mV for each, thus only 1250 steps over 6.25 s will be available. If the ramp is limited to 1.6 V the full 10 s ramp will be available.

4.5.7. Chronopotentiometry Electrodes

[61] In a chronopotentiometry (CP) measurement the potential at a working electrode is adjusted to a value to provide a specified constant current. As the current is stepped (ramped) from zero to some specified value, the potential to maintain it at that level is recorded. A detailed review of the technique is beyond the scope of this paper and reader is referred to the many texts that have been written which describe the theory and experimental practice of CP [*Bard and Faulkner*, 2001]. CP was added to the WCL to provide a secondary halide measurement technique since solutions containing mixtures of halides (Cl^-, Br^-, and I^-), may cause cross interferences on the halide ISEs and complicate the determination of individual halide concentrations.

[62] As typically implemented in a laboratory setting, the WCL CP uses either a current step or linear current ramp. A three-electrode configuration is employed, with one of the 1 mm diameter Ag electrodes serving as the anodic working electrode, the platinum ORP electrode serving as the counter electrode (as in the case for CV), and one of the chloride ISEs serving as the reference electrode. The reaction of interest occurring at the silver electrode is

$$Ag + X^- \rightarrow AgX + e^- \tag{6}$$

$$Ag(s) - e^- \rightarrow Ag^+ + X^- \rightarrow AgX \tag{7}$$
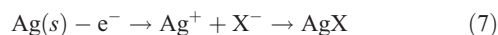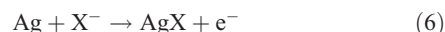
where X represents either Cl, Br, or I. The halide concentration in the bulk solution C^* can be calculated using the Sand equation, which for the current step technique can be expressed as

$$C^* = \left(2i\tau^{1/2}\right) / \left(nFAD^{1/2}\pi^{1/2}\right) \tag{8}$$

where i is the applied current, τ is the transition time, F is Faraday's constant, A is the electrode area, and D is the halide diffusion coefficient. As current is applied in a CP measurement, the potential at which reaction (6) can proceed is rapidly reached and the halide is depleted at the surface of the electrode. As the halide is depleted at the surface of the electrode, the potential required must be increased in order to allow reaction 6 to proceed and maintain the set current. When the concentration of X^- drops to zero at the electrode surface, the transition time is reached (τ) and electrode potential rapidly shifts. The potential at which a reaction occurs at the working electrode depends upon, in part, the redox potential of the process. For halide mixtures, the transition time for iodide will occur first, at the lowest potential, followed by (at higher transition times and potentials) bromide and then chloride.

[63] As is the case for CV, the measured potential of the CP transitions will be a function of solution chloride concentration and the maximum duration of a CP scan is about 12 s. An operational margin of 3 s is being used to avert the possibility of an instrument timeout, thus limiting the scan length to 9 s. For this reason, multiple CP scans at different current levels are needed to measure halides over the concentration range specified by the mission requirements.

4.5.8. Anodic Stripping Voltammetry at a Gold Microelectrode Array

[64] Anodic stripping voltammetry is an electrochemical technique capable of detecting a variety of heavy metal ion species at the ppb to ppm concentration range. The WCL uses a microfabricated array of gold microelectrodes to perform ASV analysis primarily for detection of Fe^{n+} and several other metals which may be possible poisons for several of the ISEs. Microelectrodes are used because they provide excellent background current rejection, and their small size, reproducibility, and rugged construction, makes them excellent candidates for in situ use in planetary chemical analyses. The use of microelectrodes in an array further enhances their utility by providing a low noise level, amplification of the signal, while keeping individual microelectrode behavior. The gold microelectrode array chips used in the WCL were custom fabricated (IBM Watson Research Center, Yorktown Heights, New York) and have been previously described [*Feeney and Kounaves*, 2000; *Herdan et al.*, 1998]. Each chip measures 3.1×3.4 mm and contains an array of 564 interconnected disk shaped gold microelectrodes. Each microelectrode measures 12 μm in diameter and is 66 μm (center-to-center) from its nearest neighbor.

[65] ASV is fundamentally a "preconcentration" technique in which the metal ions in the sample solution are electrochemically reduced onto an electrode surface by applying a sufficiently reducing potential. The deposition potential is limited cathodically to about -1.2 V versus SCE (saturated calomel reference electrode) by the reduction of water, and anodically to between 0.2 and 0.6 V versus SCE by the oxidation of the electrode surface or the water. After a specified deposition time, the potential is scanned in the anodic direction and the deposited metal is then oxidized (stripped) off of the electrode surface as its oxidation potential is reached. The resulting stripping peak current is proportional to the concentration of the metal ion in the sample solution and the deposition time. The position of the stripping peak is specific to the metal and the composition of the sample matrix.

4.6. Reagent Composition and Delivery

[66] To carry out the chemical analyses, the WCL includes two reagent dispensing systems: a tank containing water spiked with specific standards and five crucibles containing dry chemicals for calibration, acidification, and sulfate titration.

4.6.1. Leaching and Standards Solutions

[67] In order to provide a solvent for dissolving salts in the soil sample, the tank on the WCL (Figure 2) contains 26 mL of a solution (referred to as the "leaching solution") composed of 18 MΩ deionized water and the ten ionic species listed in Table 2. The Li$^+$ is present to provide a stable concentration for the Li$^+$ ISE that is used as a reference electrode for the other ISEs. Since a counter anion must accompany the Li$^+$, the NO_3^- is unfortunately an unwelcomed hitchhiker and increases the limit of detection (LOD) for NO_3^- to concentrations $>10^{-3}$ M (>300 ppm in the sample). The same, but not as drastic, is true for the Cl$^-$ which is used as a counter anion for several of the other salts and is present at 5×10^{-5} M. The Ca^{2+}, Mg^{2+}, K$^+$, Na$^+$, NH$_4^+$, and Ba^{2+} (used for titrimetric determination of SO_4^{2-}) are all at 1×10^{-5} M and act as the standards for the first point in the calibration of the respective ISEs on the surface of Mars. The HCO_3^- was added to stabilize the pH of the leaching solution. The leaching solution as delivered for flight has a measured electrical conductivity of 115 ± 3 μS cm^{-1} (22°C).

[68] The 26 mL of leaching solution is sealed in a 36 mL titanium tank and the 10 mL head space is filled with approximately 1000 mbar of gas with composition 0.8% CO$_2$, 94.2% N$_2$, and 5% He. This concentration of CO$_2$ and the 1×10^{-5} M of HCO$_3^-$ result in a leaching solution with an initial pH of 5.0 (5°C). By the time Phoenix is on Mars, the differential pressure between the tank head space (1000 mbar) and beaker (approximately between 0 and 100 mbar) will insure that upon puncture of the sealing disk the leaching solution will be dispensed into the beaker assembly. The expansion into the 56 mL volume (total volume = 36 mL tank + 40 mL beaker + 6 mL actuator voids − 26 mL solution), and resulting drop in P_{CO2} to approximately 2.9 mbar, will increase the pH of the leaching solution to about 5.6. Additional increases in pH to about 7 will result from the opening and closing of the WCL drawer (burping) during the analyses.

4.6.2. Second Standards Addition

[69] The first crucible in the crucible dispenser assembly contains dried salts which, when added to the leaching solution in the beaker, will act as the standards and provide a second calibration point for most of the sensors. The calibrant crucible contents were formulated from a mixture consisting of 2.0016 g ammonium nitrate (NH$_4$NO$_3$), 6.6104 g magnesium nitrate hexahydrate (Mg(NO$_3$)$_2 \cdot$ 6H$_2$O), 3.6752 g calcium chloride dihydrate (CaCl$_2 \cdot$ 2H$_2$O), 1.8642 g potassium chloride (KCl), 6.1076 g barium chloride dihydrate (BaCl$_2 \cdot$ 2H$_2$O), and 2.1003 g NaHCO$_3$. Each salt except the NaHCO$_3$, was prepared in a 25 mL solution of nano-pure H$_2$O. The NaHCO$_3$ was prepared in a 50 mL of nano-pure H$_2$O. Then 2 mL of all the solutions, except the NaHCO$_3$ (of which 4 mL was used) were combined and volumetrically diluted to 100 mL in nano-pure H$_2$O. Thirty μL of the total solution was added to each flight crucible and dried for 18 h. The resulting concentrations after the addition are shown in Table 2 under the heading TS21 for the calibration solutions used on Earth, and M-TS21 for Mars. The addition of the first crucible also increases the solution EC to 142 ± 3 μS cm^{-1} (22°C).

4.6.3. Acid Addition

[70] The second crucible in the dispenser assembly contains 0.004 g of 2-nitrobenzoic acid, which will be added to the mixture of Mars sample and solution in order to lower the pH. This addition will take place on the second day of the WCL analysis. The change in the sample pH will depend on the effects of the previous "burps" and on the pH of the Martian soil. If slightly alkaline it may provide

some indication of its buffering capacity. A slightly acid solution is also preferred for the barium titration of sulfate.

4.6.4. Barium Chloride Additions

[71] The third, fourth, and fifth crucibles each contain approximately 0.1 g of hydraulically packed dried $BaCl_2$. These crucibles will be delivered in sequence and will provide for titration of any soluble sulfate in the sample by the added Ba^{2+}. If the soil is moderately alkaline, an insoluble species such as $BaCO_3$ may also form and must be taken into account in the analysis. Previous missions indicate sulfate as the most probable titrant for barium. The addition of Ba^{2+} to a sample solution containing sulfate will form $BaSO_4$ which will then precipitate. The titration procedure will allow the concentration of sulfate to be determined by two methods.

[72] In the first method, the voltage of the Ba^{2+} ISE is monitored as an indicator of the uncomplexed Ba^{2+} remaining after the first, second, or third $BaCl_2$ crucible is added, depending on which addition is the first to produce excess Ba^{2+}. The amount of sulfate precipitated, and thus the concentration in the original sample, can be calculated from the difference between the known amount of Ba^{2+} added and the amount of unprecipitated Ba^{2+} remaining after the titration.

[73] The second method uses the voltage readings of both the Ba^{2+} and Cl^- electrodes to determine the amount of sulfate that is precipitated during the titration. If no sulfate is present in the solution, adding a $BaCl_2$ crucible will show a constant increase in the concentration of Ba^{2+} and Cl^- ions with a ratio of 1:2. In contrast, if sulfate is initially present in the solution, there will be an increase in the Cl^- concentration with no increase in the Ba^{2+} concentration since it will precipitate from solution as $BaSO_4$. Only when all of the sulfate has been precipitated will the Ba^{2+} concentration begin to increase. At this point, the ratio of Ba^{2+} to Cl^- will differ from 1:2 by an amount that is directly proportional to the amount of $BaSO_4$ precipitate formed during the titration. Accordingly, the sulfate concentration can be calculated from the voltage difference between the Ba^{2+} and Cl^- ISEs at any time after the titration is complete.

5. Calibration

[74] A total of six functional/calibration tests were performed at various stages of assembly or over time. Tests 1−3 were performed at Thermo Scientific and 4−6 at the Jet Propulsion Laboratory (JPL). The sensors were calibrated at ambient T and P. The beakers were calibrated (1) individually before integration into the beaker, (2) after integration into the beaker, (3) after thermal cycling, (4) before acceptance testing, (5) after acceptance testing, and (6) before delivery to Phoenix at Lockheed Martin. Additional calibration will be performed on Mars as part of the experimental protocol.

[75] Before integration into the flight beaker, each sensor was calibrated individually in a solution containing only the species of interest in order to avoid interferences. For the ISEs this included measuring the electrode potential in ion solutions of known concentration, against an external silver/silver chloride reference electrode.

[76] The final preflight calibration was performed on 7 March 2007, on eight candidate WCL beaker units using calibrated test bed electronics and analog boards. Four of these beakers were selected for flight based on slight differences in overall performance, and the remainder were retained for characterization, analog studies, and as witness samples. All data reported here is for the selected beaker flight units designated as 014, 018, 020, and 022.

5.1. Ion Selective Electrodes

[77] The calibrations of the ISE sensors were performed using five test solutions designated as TS20−TS24 (Table 2). The TS20 solution is the equivalent of the leaching solution as dispensed from the tank. The TS21−TS24 solutions contain the same ionic species but at increasing concentrations. With the exception of the Li^+, NO_3^-, and HCO_3^-, each ionic species is increased by three times for TS21 and 1 order of magnitude from 10^{-4} to 10^{-2} M for the others. This allowed the sensors to be tested over a significant portion of their dynamic analytical range. Since the Li^+ ISE acts as a reference electrode, the Li^+ concentration must be kept constant at 10^{-3} M. The NO_3^- was chosen both as a counter ion for the Li^+ and also the NH_4^+ and Mg^{2+}, thus its concentration increases although not in exact proportion to the other ions. The concentration of the HCO_3^- is maintained at 10^{-5} M in order to provide a constant pH during the calibration.

[78] Table 3 gives the results of two of the five calibrations, before shipping at Thermo, and the final test at JPL, for eight of the ISEs using solutions TS20−24 in each of the flight beakers (014, 018, 020, and 022). The differences among the beaker ISEs over the test duration and their standard deviations are shown in Table 4. As can be seen by the standard deviation, the individual ISEs show similar values for the intercept ($E°$) and the slope (S). The Br^- and I^- ISEs were not calibrated after integration, since addition of the respective ions would damage the Cl^- ISE.

[79] The ISEs will also be calibrated in situ on Mars before soil addition. The calibration is effected by providing two points via the addition of the leaching solution and the first reagent crucible.

5.2. Hydrogen Ion Activity

[80] Prior to integration into the flight beaker assembly, all pH sensors were tested using a series of Thermo-Fisher pH standards (pH 1.68, 4.01, 6.86, 7.00, 10.01). Table 5 shows the test data for all three pH sensors integrated into flight beaker 014 which is representative of the data for all the flight sensors. After integration into the beaker and during the testing of the ISE sensors discussed above (section 5.1), the output of the pH sensors was also recorded. However, the pH in the five test solutions (TS20−TS24) varies by less than a pH unit and these tests provided more of a functional test than a calibration test. Because of concern of contamination of the beaker sensors, only test solutions TS20−TS24 were allowed in the flight beakers. The pH range of the TS21 solution was extended slightly by saturating the solution with air and with 5% CO_2 for a pH of 6.60 and 5.00, respectively, as measured against an external calibrated commercial pH meter. The slope and intercept for all of the pH sensors in all flight beakers from the final calibration data set using air and CO_2 saturated TS21 solution is summarized in Table 6. On Mars,

Table 3. Intercept $E°$ and Slope S of Five Calibrations for Flight Units

	Thermo (After Integration)							
	Beaker 020 on 8 Aug 2006		Beaker 018 on 8 Aug 2006		Beaker 022 on 8 Aug 2006		Beaker 014 on 8 Aug 2006	
	Slope (mV decade^{-1})	Intercept (mV)	Slope (mV decade^{-1})	Intercept (mV)	Slope (mV decade^{-1})	Intercept (mV)	Slope (mV decade^{-1})	Intercept (mV)
Na^+	54.4	170	53.0	163	53.7	173	54.2	202
NH_4^+	58.9	184	57.5	169	58.4	182	58.4	171
K^+	58.7	172	57.5	166	58.6	174	58.8	176
Ca^{2+}	29.3	144	28.9	139	28.6	139	28.8	141
Mg^{2+}	28.8	138	28.0	122	28.9	140	29.0	145
Ba^{2+}	29.9	220	29.1	213	29.6	225	29.5	227
NO_3^-	−58.3	70.2	−58.5	60.4	−58.9	69.4	−57.8	65.9
Cl^-	−54.9	49.6	−54.6	44.7	−54.4	49.9	−55.5	47.1
	JPL (Final)							
	Beaker 020 on 6 Mar 2007		Beaker 018 on 6 Mar 2007		Beaker 022 on 6 Mar 2007		Beaker 014 on 6 Mar 2007	
	Slope (mV decade^{-1})	Intercept (mV)	Slope (mV decade^{-1})	Intercept (mV)	Slope (mV decade^{-1})	Intercept (mV)	Slope (mV decade^{-1})	Intercept (mV)
Na^+	53.7	177	53.6	178	54.6	183	54.7	220
NH_4^+	61.0	192	59.8	178	60.3	189	60.6	187
K^+	59.7	174	60.9	177	59.1	178	59.3	181
Ca^{2+}	29.4	145	29.5	147	29.2	143	29.3	146
Mg^{2+}	28.9	139	28.0	129	28.8	142	28.5	145
Ba^{2+}	30.4	219	29.6	213	30.2	221	30.2	226
NO_3^-	−57.7	56.6	−58.0	57.3	−57.6	66.8	−58.8	60.1
Cl^-	−55.4	49.0	−54.6	50.0	−54.0	50.5	−55.5	48.0

two in situ calibration points will be collected before the addition of soil.

5.3. Conductivity

[81] Prior to integration of the conductivity sensors into the flight beakers, each sensor was tested using commercial Thermo-Fisher conductivity standards (100, 1413, 12.9, and 111.9 mS cm^{-1}). After integration into the flight beakers, the output of the conductivity sensors were monitored during the testing of the ISE sensors at various stages of assembly as discussed in section 5. The final test was performed following acceptance testing using the test solutions TS20–24, which cover the conductivity range 118 to 9620 μS cm^{-1} as measured against an external calibrated commercial conductivity sensor. All sensors demonstrated expected linearity over the tested range.

5.4. Redox Potential: E_h

[82] Prior to integration into the flight beaker, all ORP sensors were tested in commercial ORP standards and showed excellent response. After integration into the beakers, the outputs of the ORP sensors were monitored during the testing of the ISE sensors.

5.5. Cyclic Voltammetry

[83] Prior to integration of the CV electrodes into the flight beakers, the Au working electrodes were polished and

tested in a 5 mM $K_3Fe(CN)_6$; 5 mM $K_4Fe(CN)_6$; 0.1 M KNO_3 solution using a Pt wire as a counter electrode and an Orion 9002 Ag/AgCl reference electrode. All the electrodes performed satisfactorily. Because of contamination concerns, once the CV electrodes were integrated into the flight beakers, only functional tests, using the ISE calibration solutions, were performed. Tests using solutions that contained strong redox couples (e.g., $K_3Fe(CN)_6/K_4Fe(CN)_6$) were avoided. After delivery of the flight beakers to JPL, the CV electrodes were tested for functionality in TS21 in August 2006, December 2006, and February 2007 at the time of ISE calibration. The number of functional test scans was limited (typically three scans over the range of −1 to 1 V at approximately 300 mV s^{-1}) to prevent any undesirable effects on the Au electrode surface.

5.6. Chronopotentiometry

[84] Prior to flight, CP test scans were performed in TS20 (leaching solution) and TS21 (calibrant solution). To prevent irreversible changes in the CP silver working electrodes, the number of scans run prior to flight were kept to a minimum. Representative scans in TS21 for each of the flight beaker electrodes are shown in Figure 13. The results of three anodic scans run in TS20 (5×10^{-5} M Cl^-) and three anodic scans run in TS21 (1.5×10^{-4} M Cl^-) for each electrode are summarized in Table 7. The uncorrected % error for scans taken in TS20 ranged from approximately 2 to −20% and 4 to −10% for scans taken in TS21 (excluding outlying values for

Table 4. Differences Among the Flight Beaker ISEs Over the Test Duration for the Intercept $E°$ and the Slope S

ISE	Average $E°$ (mV)	SD	Average S (mV 10^{-1})	SD
Mg	135	4	27.6	1.6
Ca	141	4	28.1	1.7
K	170	7	57.2	3.0
Ba	219	5	29.0	1.8
NH$_4$	181	8	58.4	3.1
Na	181	6	52.7	2.4
Cl	50	2	−54.3	1.3
NO$_3$	63	5	−58.5	0.5

Table 5. Test Results for pH Sensors for WCL Beaker 014

	mV Versus Ag/AgCl		
pH	pH 1 Polymer	pH 2 Polymer	Ir oxide
1.68	269	273	514
4.01	135	138	377
6.86	−27	−23	-
7.00	-	-	186
10.0	−157	−151	−38

Table 6. Calibration Constants for pH Sensors in Each Flight Beaker

	Beaker							
	014		018		020		022	
	Slope (mV pH^{-1})	Intercept (mV)	Slope (mV pH^{-1})	Intercept (mV)	Slope (mV pH^{-1})	Intercept (mV)	Slope (mV pH^{-1})	Intercept (mV)
Ir oxide	−58.7	655	−56.4	578	−52.4	610	−52.4	611
pH 1 (upper)	−54.6	383	−59.3	402	−56.0	371	−58.1	399
pH 2 (lower)	−56.1	395	−59.7	407	−57.2	388	−55.8	372

the beaker 014 Ag-1 electrode). The chloride concentrations determined with the beaker 014 Ag-1 electrode were anomalously high. The cause of this error is unclear but may be due to a higher level of electrode charging compared to the other silver electrodes. The higher error for scans taken in TS20 is expected. In general, at lower chloride concentrations (shorter transition times), measurement errors increase.

[85] CP calibration scans will be run in both leaching solution and calibrant solution on Mars. With the data from these scans, we will use a standard method [*Bard*, 1963] to correct for double-layer effects and other sources of error. In this approach,

$$i\tau/C_o^* = a + b/C_o^*\tau^{1/2} \qquad (9)$$

where C_o^* is the bulk concentration, a equals $nFAD_o^{1/2}\pi^{1/2}/2$ and b represents a correction factor. The parameter a, which is sometimes referred to as the chronopoteniometric constant, represents a correction for non-Faradaic electrode processes and the difference between measured and effective electrode areas. By determining the transition time (τ) at multiple known current values on Mars, both a and b can be determined from a plot of $\tau^{1/2}$ versus $i\tau$. After applying this correction and considering possible interferences (section 6.7), we anticipate that the concentration measurement error for halides in solution will not exceed ±20%.

6. Characterization

[86] The WCL was characterized in order to determine the full capabilities or limitations of all the sensors and subsystems, and to anticipate operation in the Martian environment. This section covers the characterization of all the sensors in the WCL beaker and actuator assembly, describing those results as well as information relevant to the operation and measurements to be obtained on Mars. Because of complexity and cost, characterizations were performed using either an Engineering Qualification model (EQM), the heritage beakers from MSP'01, or six specially built test bed units that resemble the flight hardware in ways adequate for testing, but do not necessarily share form, fit, and total function, and are not packaged for vacuum use or complete hermeticity. Essential functions were then reproduced with flight-like electronics and software to verify that the test bed results are representative of the performance expected on Mars.

[87] The test bed units contain a flight equivalent epoxy cup with all the sensors on the internal walls configured as the flight beakers. The epoxy cups however are not surrounded by the electronics cards or the potting epoxy. The cups are mounted on PC boards containing the

preamplifier electronics, enclosed within an aluminum casing, and controlled by a flight-like analog electronics board. The WCL is normally controlled by the MECA CME board. However, for the purposes of characterization where the emphasis is sensor performance, the CME and power board functions were simulated, an external stirrer was used for mixing, and sensor control and measurement was performed by a desktop computer using LabView software.

6.1. Ion Selective Electrodes

[88] Characterization of the ISEs was accomplished by running calibration curves under a variety of conditions and background matrices. These included extremes in ionic strength, pH, temperature, and backgrounds of ionic species which might be found at significant concentrations in a Martian sample such as Na^+, K^+, Ca^{2+}, Mg^{2+}, Cl^-, SO_4^{2-}, $Fe^{3/2+}$. Several other characterizations, such as particle size-membrane interaction, are still in progress.

[89] Calibration curves were obtained by starting with a concentration of 10^{-5} M of each ion being measured by an ISE. The TS20 solution (Table 2) was modified by adjusting pH, heating, cooling, or adding ions to it, as required to meet the specific test conditions. Small spikes of 0.1 M solutions of Na^+, K^+, NH_4^+, Mg^{2+}, Ca^{2+}, Ba^{2+}, Cl^-, and NO_3^-, containing the background or condition being tested
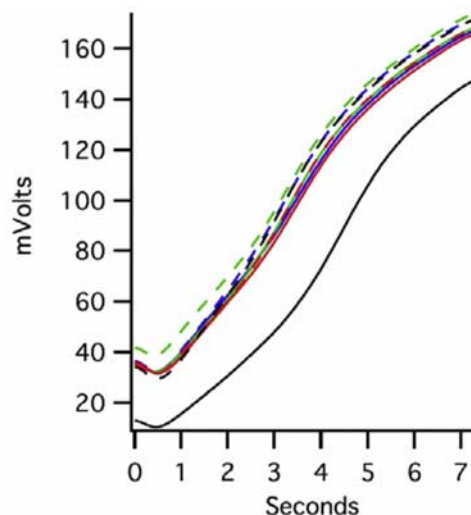

Figure 13. Beaker 020 Ag-1 is the solid green curve, beaker 020 Ag-2 is the green dashed curve, beaker 018 Ag-1 is the solid blue curve, beaker 018 Ag-2 is the blue dashed curve, beaker 022 Ag-1 is the solid red curve, beaker 022 Ag-2 is the red dashed curve, beaker 014 Ag-1 is the solid black, and beaker 014 Ag-2 is the black dashed curve. Potential is referenced against the Cl^- ISE.

Table 7. Average of Three Scans for Chloride Concentration in TS20 and TS21

Beaker Serial Number	Electrode	TS20 Measured (mol L^{-1})	σ	Average Error (%)	TS21 Measured (mol L^{-1})	σ	Average Error (%)
020	Ag-1	5.11×10^{-5}	9.1×10^{-6}	2.15	1.41×10^{-4}	1.8×10^{-6}	−6.13
020	Ag-2	4.36×10^{-5}	0	−12.71	1.41×10^{-4}	4.6×10^{-6}	−6.21
018	Ag-1	4.66×10^{-5}	1.3×10^{-6}	−6.88	1.56×10^{-4}	1.9×10^{-6}	3.72
018	Ag-2	4.10×10^{-5}	5.2×10^{-6}	−18.1	1.39×10^{-4}	1.1×10^{-5}	−7.56
022	Ag-1	5.04×10^{-5}	9.8×10^{-6}	0.71	1.50×10^{-4}	1.8×10^{-6}	0.17
022	Ag-2	4.46×10^{-5}	9.9×10^{-6}	−10.8	1.45×10^{-4}	5.4×10^{-6}	−5.42
014	Ag-1	5.47×10^{-5}	4.0×10^{-6}	9.33	2.32×10^{-4}	5.7×10^{-6}	54.3
014	Ag-2	4.02×10^{-5}	4.2×10^{-6}	−19.5	1.35×10^{-4}	4.7×10^{-6}	−10.2

for, were added to progressively increase the concentration of ions of interest to 10^{-4} M, 10^{-3} M, and 10^{-2} M. Occasionally, it was possible to obtain additional calibration points, but calibration curves were never determined with less than four points. The calibration curves obtained under these various conditions were then compared to calibration curves obtained in the unmodified series of TS solutions.

6.2. Effects of Ionic Strength

[90] If a sample of Martian regolith containing high levels of soluble salts is delivered to the WCL, the increased ionic strength (μ) of the solution would change the activity (effective concentration) of all ionic species. This effect becomes noticeable for solutions with $\mu > 10^{-4}$ M. The most significant effect of increased ionic strength will be on the ISE sensors. The response of an ISE is described by the Nernst equation (equation (1)) such that the potential of the ISE is dependent on the activity of the primary ionic species. Changes in μ will have a direct effect on the measured potential of the ISEs and thus it is important to understand the behavior of the ISEs in solutions containing a high total concentration of ionic species.

[91] To test for the effect of increased ionic strength on the ISEs, it is necessary to use an ion which will increase μ but not be detected by the ISE either as a primary or interferent ion. $Be(NO_3)_2$ was used since neither Be^{2+} nor NO_3^- were found to significantly interfere with any of the cationic ISEs. It was added to the test solutions at concentrations of 10^{-5} M, 10^{-4} M, 10^{-3} M, 10^{-2} M, and 10^{-1} M. The responses for all ISEs were Nernstian (Table 8).

6.3. Effects of Hydrogen Ion Concentration

[92] Since the pH of the Martian regolith has never been directly measured, delivery of a sample on Mars to the WCL could result in a solution of extreme pH values. A very high or low pH might not only affect the ISE membrane and ionophore chemistry, but could also physically alter or irreversibly damage it. To test for such effects, the ISEs were calibrated in solutions covering a range from pH 1 to pH 12.

[93] For calibrations in solutions of pH 3 through pH 10, the ISEs responded in a Nernstian manner with slopes close to the expected values. However, at very acidic pHs of 1 and 2, as well as very basic pHs of 11 and 12, most all ISEs exhibited a significant decrease in sensitivity and in some case no obvious response at all or with slopes of opposite sign. The only ISE which did not seem to be affected as drastically was the NH_4^+ ISE. The results are shown in Table 9.

6.4. Effects of Temperature

[94] The effect of temperature on the sensitivity (S) of an ISE is given by the Nernst equation (equation (1)) as $\Delta S = 0.20$ mV °C^{-1} for z = 1 (at 5°C, $S = 55.2$ mV and at 20°C, $S = 58.1$ mV), and thus there is a slight loss of sensitivity as temperatures decrease. Even though such temperature effects can be calculated, the ISEs were tested at various temperatures to insure that non-Nernstian processes, such as restricted diffusion or membrane instability did not produce additional changes.

[95] Calibration curves were obtained using TS20–TS24 solutions at temperatures from 2 to 40°C (see Table 10). A very slight loss of sensitivity is expected at lower temperatures from the Nernstian behavior of ISEs. The results showed very little change of the calibration over this temperature range and the ISEs performed as expected at the temperatures to be encountered during operations on Mars.

6.5. Effects of Ammonium

[96] The effects of a high concentration of NH_4^+ on the WCL sensors were characterized because NH_3, a decomposition byproduct of the hydrazine Lander thruster engines, could possibly contaminate the soil at the landing site, and upon addition of a sample to the cell, generate NH_4^+. The levels of NH_4^+ will be determined by the NH_4^+ ISE. The interference of NH_4^+ on the other ISEs, was tested by adding sufficient NH_4NO_3 to the TS21 solution to give 1×10^{-5}, 3×10^{-5}, 10^{-4}, 10^{-3}, and 10^{-2} M NH_4^+. The effects, were minimal over the entire range with only a 5–10 mV level of interference for all the ISEs. At the 10^{-2} M level, the K^+ and Na^+ ISEs exhibited about a 45 mV and 30 mV interference, respectively.

6.6. Cyclic Voltammetry

[97] A number of factors, including formation of oxides and adsorbed organic films, may adversely affect the CV electrodes prior to use during surface operations. Since electrode performance can degrade with repeated cycling,

Table 8. Effect of Ionic Strength μ on ISE Slopes[a]

	$\mu = 10^{-4}$ M	$\mu = 10^{-3}$ M	$\mu = 10^{-2}$ M	$\mu = 10^{-1}$ M
Ba^{2+}	24.2	25.7	27.5	29.7
Ca^{2+}	22.0	19.8	18.6	-
K^+	48.4	48.8	49.0	52.9
Mg^{2+}	-	-	-	-
Na^+	49.7	54.0	55.3	54.0
NH_4^+	53.7	52.0	56.0	48.6

[a]ISE slopes are in units of mV decade^{-1}.

Table 9. Effect of pH on ISE Slopes[a]

	pH 1	pH 2	pH 3	pH 4	pH 5	pH 6	pH 8	pH 9	pH 10	pH 11	pH 12
Ba^{2+}	−0.4	−8.8	28.2	28.5	29.3	29.0	29.1	29.4	29.1	23.7	−7.5
Ca^{2+}	-	-	28.9	29.5	29.4	28.3	26.9	26.2	27.0	-	-
K^+	39.5	53.7	51.0	50.0	44.3	58.2	53.7	52.9	63.5	20.3	7.4
Mg^{2+}	0.7	1.8	23.8	27.3	27.9	26.8	26.8	26.7	27.3	17.0	5.5
Na^+	-	-	41.2	42.2	39.9	47.68	45.2	43.6	43.5	-	-
NH_4^+	48.0	52.9	52.4	55.1	53.7	59.3	46.1	58.6	54.7	56.5	35.4
NO_3^-	-	-	-	−56.5	−59.6	−61.4	−50.2	−48.5	−51.2	-	-
Cl^-	-	-	−56.2	−56.7	−55.5	−58.6	−53.7	−56.9	−59.6	-	-

[a]ISE slopes are in units of mV decade^{-1}.

the number of CV scans performed with the flight electrodes after they were polished and integrated into the WCL beakers resulted in a very limited ability to characterize the CV electrodes. To compensate for the limited characterization and any adverse preflight effects, an electrode conditioning sequence for Mars operations was validated. The sequence anodically scans the electrode potential above +1 V to form a gold oxide film, then cathodically scans to −1 V to reduce the electrode surface back to Au. Cycling the scan in this manner also helps destroy other contaminants that may be covering the electrode. During surface operations, the position of the Au oxidation and reduction peaks, which occur at known potentials, can be used to establish the chloride reference offset of the CV scan relative to standard electrode potentials. Figure 14 shows the performance of the CV working electrode before and after conditioning in a TS21 solution containing 1×10^{-3} M FeSO$_4$.

6.7. Chronopotentiometry

[98] Characterization tests showed that SO_4^{2-} and Fe^{3+} do not cause significant interference in the determination of halides by CP in the WCL. High NH_4^+ concentrations (0.01 M) appear to cause interference, however, the chloride concentrations in NH_4^+ containing solutions are correctable to approximately 2% using the method described in section 5.6. In basic solutions (>pH 9) the presence of OH^- causes significant interference through the formation of silver oxide. In a pH 6 solution, calculation of the chloride concentration (1.5×10^{-4} M) based on the observed transition time yielded an error of approximately 2%, while in the pH 10 solution, no transition time was observed. If a soil sample with a basic pH is analyzed on Mars, CP could still successfully be used to determined halide concentrations if the acid addition brings the sample pH into the neutral or acid range. After addition of acid, on the basis of the observed transition times, the measured concentrations at pH 6 and 10 were 0.147 mM and

0.143 mM, respectively, while the actual concentration was 0.150 mM.

[99] Overall, mixtures of halides can be determined with an error of 2−20%, depending the relative concentrations. The minimum detectable level of Cl^-, Br^-, or I^- is 5×10^{-5} M. As concentration ratios increase the minimum detectable halide level increases. However, if the lower concentration component in a halide mixture is not detected, no significant error is introduced to the measurement of the dominant halide species (most likely chloride). In this case, the CP determined Cl^- concentration can be used to correct the halide ISE measurements.

7. Analytical Protocol

[100] The procedure for a nominal two sol chemical analysis is shown in Figure 15. The process on the first sol (sol A) is initiated by melting the frozen leaching solution in the reservoir, a process that may take up to 90 min. When completely melted, as indicated by the external tank temperature, the seal on the water tank is punctured and the 1 bar N$_2$/CO$_2$ gas mixture sealed in the tank headspace forces the solution into the beaker. The leaching solution contains the dissolved salts that provide the required ions for the first calibration point for the ISEs. The temperature in the beaker is maintained at $7 \pm 0.5°C$

Table 10. Effect of Temperature on ISE Slopes[a]

	2°C	5°C	15°C	24°C	30°C	40°C
Ba^{2+}	27.0	28.7	29.2	29.1	30.3	30.7
Ca^{2+}	22.6	25.1	27.8	29.9	29.0	29.5
K^+	50.5	55.4	56.8	58.3	60.9	64.3
Mg^{2+}	22.0	23.9	26.1	28.7	27.9	30.1
Na^+	44.0	47.5	45.6	47.9	47.4	47.9
NH_4^+	53.4	58.5	56.1	59.3	61.0	63.6
NO_3^-	−58.8	−59.7	−59.4	−58.3	−60.3	−63.2
Cl^-	−45.1	−50.0	−50.9	−52.4	−56.3	−57.6

[a]ISE slopes are in units of mV decade^{-1}.
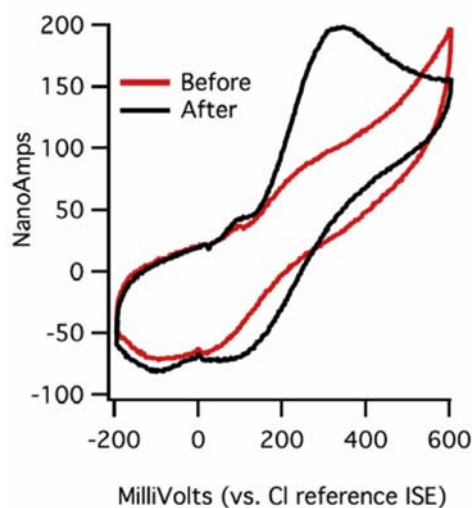

Figure 14. Cyclic voltammograms obtained using 1×10^{-3} M FeSO$_4$ (TS21 background) before (red curve) and after conditioning (black curve). Potential is referenced against the Cl^- ISE.
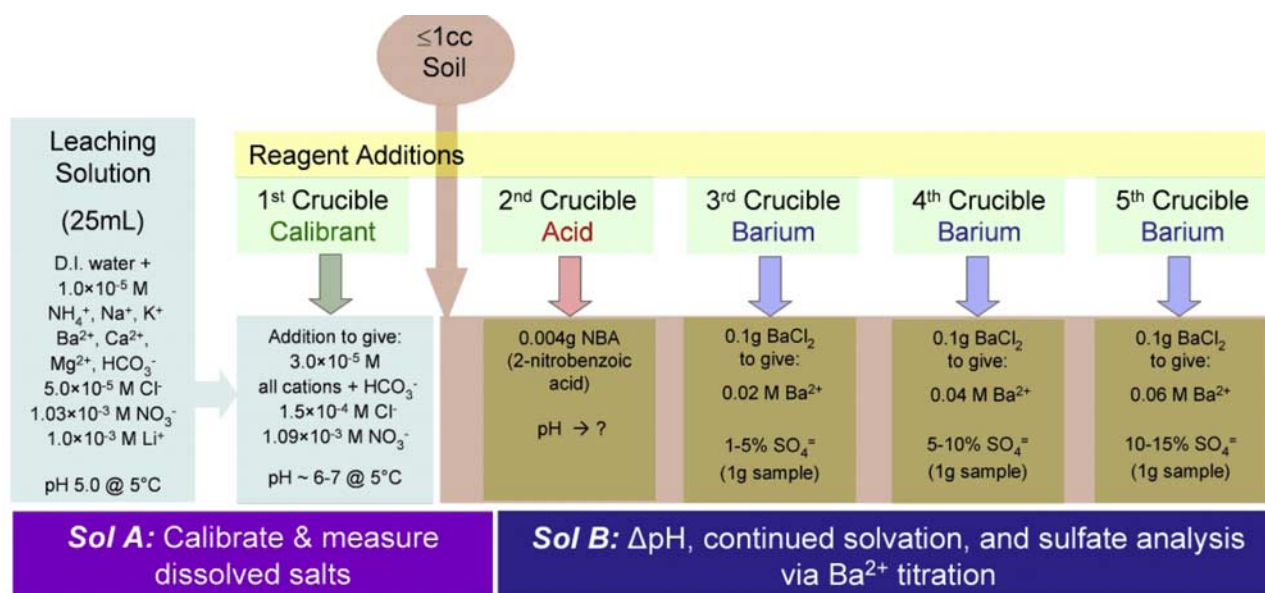
Figure 15. Diagram of analytical protocol. The exact pH after the first crucible addition will depend on the number of drawer open/close cycles and remaining CO_2 in the head space. The pH after the acid addition will depend on the pH and buffering capacity of the Martian soil sample.

during the sol A analyses, typically oscillating over that range with a time constant of several minutes.

[101] Positive pressure inside the WCL can be relieved by cycling the sample drawer open and closed. The intermediate position between open and closed allows gas exchange between the inside and the outside for several seconds. Typically, this is done with the solution temperature slightly above the external boiling point of approximately 7°C, resulting in reduction of the internal pressure to that generated by the water vapor. This process drives other gases from the headspace that might impede the dissolution of the material in the crucibles by forming gas bubbles.

[102] The solution is monitored for a 15 min equilibration period prior to the first drawer open/close cycle, which will relieve approximately 200 mbar of residual gases that expanded from the head space in the solution storage tank. The first crucible is then released to provide the salts for the second calibration point. The sensors are monitored for an additional 30 min prior to soil sample addition.

[103] The analysis of the soil sample is initiated with the opening of the drawer, whereupon the Lander's robotic arm delivers the soil sample into the funnel that feeds the 1 cm^3 sample receptacle. Documentation by the robotic arm camera (RAC) will allow the volume to be estimated to an accuracy of approximately 0.25 cm^3. The drawer is then closed and the sample dispensed into the beaker. A second drawer opening and closing allows additional images to be acquired to determine whether the sample was successfully delivered, simultaneously removing particles from the drawer sealing surface that might otherwise allow excessive evaporation of the solution during the subsequent analysis. The end-to-end sample delivery process takes approximately 40 min.

[104] For the remainder of the available analysis time, an estimated 200 min, the solution is monitored by a choreographed program of sensor measurements, stirring, and

voltammetric or potentiometric ramps, all while maintaining the beaker temperature at approximately 7°C. The actual available operating time is determined by the spacecraft energy budget. At the end of that time the power is switched off and the WCL is allowed to freeze overnight.

[105] The second sol (sol B) starts with the thawing of the solution in the beaker, up to 90 min, followed by an additional 50 min of monitoring to determine any changes in the solution or sensors resulting from the freeze/thaw cycle. A drawer cycle to purge headspace gases is followed by the addition of the acid-containing crucible.

[106] The solution is then monitored as on sol A for at least 90 min. The final analysis is the Ba^{2+} titration for sulfate. This is accomplished by sequentially dispensing crucibles 3, 4, and 5 over a 45 min period, then monitoring the sensors for at least 90 min more.

[107] The sensor array and protocol in place should allow the WCL on the Phoenix to perform a reasonably reliable chemical analysis of the soil on Mars. It will provide, taking into account the constraints of the experiments, the first ever measurements of the soil properties when mixed with water, including such parameters as pH, redox potential, and conductivity, in addition to the identity and concentration of many common ionic species.

References

Bard, A. J. (1963), Correction for the inconstancy of the chronopotentio- metric constant at short transition times, *Anal. Chem.*, *35*, 340–343, doi:10.1021/ac60196a021.

Bard, A. J., and L. R. Faulkner (2001), *Electrochemical Methods: Fundamentals and Applications*, 2nd ed., John Wiley, New York.

Bibring, J.-P., et al. (2005), Mars surface diversity as revealed by OMEGA/Mars Express, *Science*, *307*, 1576–1581, doi:10.1126/science.1108806.

Carr, M. H. (1996), *Water on Mars*, Oxford Univ. Press, Oxford, U. K.

Catling, D. (1999), A chemical model for evaporites on early Mars: Possible sedimentary tracers of the early climate and implications for exploration, *J. Geophys. Res.*, *104*, 16,453–16,469, doi:10.1029/1998JE001020.

Clark, B. C., and D. Van Hart (1981), The salts of Mars, *Icarus*, *45*, 370–378, doi:10.1016/0019-1035(81)90041-5.

Clark, B. C., A. K. Baird, R. J. Weldon, D. M. Tsusaki, L. Schnabel, and M. P. Candelaria (1982), Chemical composition of Martian fines, *J. Geophys. Res.*, *87*(B12), 10,059–10,067, doi:10.1029/JB087iB12p10059.

Clark, B. C., L. Mason, and P. Thompson (1995), Mars aqueous chemistry experiment (MACE), technical report, Lockheed Martin Astronaut., Denver, Colo.

Clark, B. C., et al. (2005), Chemistry and mineralogy of outcrops at Meridiani Planum, *Earth Planet. Sci. Lett.*, *240*, 73–94, doi:10.1016/j.epsl.2005.09.040.

Clark, B. C., A. Yen, and Athena Science Team (2006), Model for volatile incorporation into soils and dust on Mars, *Eos Trans. AGU*, *86*(52), Fall Meet. Suppl., Abstract P43A-04.

Clark, B. C., et al. (2007), Evidence for montmorillonite or its compositional equivalent in Columbia Hills, Mars, *J. Geophys. Res.*, *112*, E06S01, doi:10.1029/2006JE002756.

Dreibus, G., J. Brückner, and H. Wänke (2000), Phosphorus in Martian rocks and soils and the global surface chemistry of Mars as derived from APXS on Pathfinder, *Lunar Planet. Sci. Conf.*, *XXXI*, 1127.

Feeney, R., and S. P. Kounaves (2000), On-site analysis of arsenic in groundwater using a microfabricated gold ultramicroelectrode array, *Anal. Chem.*, *72*, 2222–2228, doi:10.1021/ac991185z.

Frant, M. S. (1997), Where did ion selective electrode come from, *J. Chem. Educ.*, *74*, 159–166.

Fry, C. H., and S. E. M. Langley (2002), *Ion-Selective Electrodes for Biological Systems*, CRC Press, Boca Raton, Fla.

Gellert, R., et al. (2004), Chemistry of rocks and soils in Gusev crater from the alpha particle X-ray spectrometer, *Science*, *305*, 829–832, doi:10.1126/science.1099913.

Grotzinger, J. P., et al. (2005), Stratigraphy and sedimentology of a dry to wet eolian depositional system at Meridiani Planum, Mars, *Earth Planet. Sci. Lett.*, *240*, 11–72, doi:10.1016/j.epsl.2005.09.039.

Herdan, J., R. Feeney, S. P. Kounaves, A. F. Flannery, C. W. Storment, G. T. A. Kovacs, and R. B. Darling (1998), Field evaluation of an electrochemical probe for in situ screening of heavy metals in groundwater, *Environ. Sci. Technol.*, *32*, 131–136, doi:10.1021/es970389z.

Kounaves, S. P., et al. (2003), Mars Surveyor Program '01 Mars Environmental Compatibility Assessment Wet Chemistry Lab: A sensor array for chemical analysis of the Martian soil, *J. Geophys. Res.*, *108*(E7), 5077, doi:10.1029/2002JE001978.

Lukow, S. R., and S. P. Kounaves (2005), Analysis of simulated Martian regolith using an array of ion selective electrodes, *Electroanalysis*, *17*, 1441–1449, doi:10.1002/elan.200503292.

McLennan, S. M., et al. (2005), Provenance and diagenesis of the evaporite-bearing Burns formation, Meridiani Planum, Mars, *Earth Planet. Sci. Lett.*, *240*, 95–121, doi:10.1016/j.epsl.2005.09.041.

Ming, D. W., et al. (1998), PHEEMS: A Mars soil reactivity experiment, *Lunar Planet. Sci.*, *XXIX*, Abstract 1232.

Ming, D. W., et al. (2006), Geochemical and mineralogical indicators for aqueous processes in the Columbia Hills of Gusev crater, Mars, *J. Geophys. Res.*, *111*, E02S12, doi:10.1029/2005JE002560.

Murchie, S., et al. (2007), Compact Reconnaissance Imaging Spectrometer for Mars (CRISM) on Mars Reconnaissance Orbiter (MRO), *J. Geophys. Res.*, *112*, E05S03, doi:10.1029/2006JE002682.

Oyama, V. I., B. J. Berdahl, and G. C. Earle (1977), Preliminary findings of the Viking gas exchange experiments and a model for Martian surface chemistry, *Nature*, *265*, 110–114, doi:10.1038/265110a0.

Quinn, R. C., P. Ehrenfreund, F. J. Grunthaner, C. L. Taylor, and A. P. Zent (2007), Decomposition of aqueous organic compounds in the Atacama Desert and in Martian soils, *J. Geophys. Res.*, *112*, G04S18, doi:10.1029/2006JG000312.

Rieder, R., T. Economou, H. Wanke, A. Turkevich, J. Crisp, J. Bruckner, G. Dreibus, and H. Y. McSween Jr. (1997), The chemical composition of Martian soil and rocks returned by the mobile alpha proton X-ray spectrometer: Preliminary results from the X-ray mode, *Science*, *278*, 1771–1774, doi:10.1126/science.278.5344.1771.

Rieder, R., et al. (2004), Chemistry of rocks and soils at Meridiani Planum from the alpha particle X-ray spectrometer, *Science*, *306*, 1746–1749, doi:10.1126/science.1104358.

Smith, P. H., et al. (2008), Introduction to special section on the Phoenix Mission: Landing Site Characterization Experiments, Mission Overviews, and Expected Science, *J. Geophys. Res.*, *113*, E00A18, doi:10.1029/2008JE003083.

Squyres, S. W., et al. (2006), Rocks of the Columbia Hills, *J. Geophys. Res.*, *111*, E02S11, doi:10.1029/2005JE002562.

Wang, M., S. Yao, and M. Madou (2002), A long-term stable iridium oxide pH electrode, *Sens. Actuators B*, *81*, 313–315, doi:10.1016/S0925-4005(01)00972-8.

Wang, A., et al. (2006), Sulfate deposition in subsurface regolith in Gusev crater, Mars, *J. Geophys. Res.*, *111*, E02S17, doi:10.1029/2005JE002513.

Yen, A. S., et al. (2008), Hydrothermal processes at Gusev crater: An evaluation of Paso Robles class soils, *J. Geophys. Res.*, *113*, E06S10, doi:10.1029/2007JE002978.

————————————

C. A. Cable, K. Gospodinova, P.-C. Hsu, J. Kapit, S. P. Kounaves, S. Stroble, and S. M. M. Young, Department of Chemistry, Tufts University, 62 Talbot Avenue, Medford, MA 02155, USA. (samuel.kounaves@tufts.edu)

B. C. Clark, Lockheed Martin Corporation, 12999 West Deer Creek Canyon Road, Littleton, CO 80127, USA.

A. Fisher, P. Grunthaner, M. H. Hecht, J.-M. Morookian, and M. Weilert, Jet Propulsion Laboratory, California Institute of Technology, 4800 Oak Grove Drive, Pasadena, CA 91109, USA.

D. W. Ming, Johnson Space Center, NASA, 2101 NASA Parkway, Houston, TX 77058, USA.

R. Quinn, SETI Institute, 515 North Whisman Road, Mountain View, CA 94043, USA.

P. H. Smith, Lunar and Planetary Laboratory, University of Arizona, 1629 East University Boulevard, Tucson, AZ 85721, USA.

X. Wen, Thermo Fisher Scientific, 166 Cummings Center, Beverly, MA 01915, USA.

S. J. West, Invensys Corporation, Foxboro Field Devices Division, 33 Commercial Street, Foxboro, MA 02035, USA.